performed qPCR assays as described previously [Sun et al., 2008] in two affected persons, III-5 (with tibial hypoplasia) and IV-3, using a cut-off RCN of 1.3; we identified a duplication of at least 105 kb spanning from nt. 156232366 to nt. 156337864 which contains *ZRS* (Fig. 1A).

Our multiple qPCR assays detected the minimal duplication but could not give precisely the breakpoints in the case. Therefore, we performed copy number and LOH analyses on three samples of IV-1 (with tibial hypoplasia), IV-3 and IV-2 (unaffected) using Illumina HumanHap550-Duo (http://www.Illumina.com). A duplication covering a 97-kb segment from nt. 156240230 to nt. 156336835 and involving *LMBR1* (Fig. 1B) was found in both patients, while no copy number variant in this region was detected in IV-3. Two SNPs flanking both sides of the duplication, rs6956930 (nt. 156230391) and rs2365750 (nt. 156345168), are not duplicated, indicating the centromeric breakpoint region of 1.975 kb from nt. 156230391 to nt. 156232366, and the telomeric breakpoint region of 7.3 kb from nt. 156337864 to nt. 156345168.

Based on the observations of an SD4 family, Rambaud-Cousson et al. [1991] suggested that SD4 is in fact a complex entity which can include a variety of lower limb malformations in addition to its typical abnormalities. We also suggested previously that SD4 with tibial hypoplasia might be a severe clinical subtype of SD4 [Sato et al., 2007], which has been genetically confirmed in the present study. Moreover, three abnormalities, that is, triphalangeal thumb, mirror polydactyly and tibial hemimelia tend to overlap among SD4, PPD, TPTPS, THPTTS (tibial hemimelia polysyndactyly triphalangeal-thumb syndrome) and mirror polydactyly with tibial hemimelia, all of which have been mapped to 7q36 [Heutink et al., 1994; Tsukurov et al., 1994; Zguricas et al., 1999]. Therefore, Kantaputra and Chalidapong [2000] proposed that THPTTS, TPTPS, PPD-2/3, and Haas-type syndactyly (SD4) are pathogenetically related. Our work, together with these previous reports [Lettice et al., 2003; Klopocki et al., 2008; Sun et al., 2008], confirmed that TPTPS and SD4 are allelic with PPD2/PPD3 (Table I) and indicated that THPTTS, TPTPS, PPD-2/3, and SD4 represent a phenotypic spectrum caused by various mutations of *SHH* or its regulator, *ZRS*.

Recently, various genomic duplications involving *ZRS* have been reported in seven families with TPTPS and/or SD4 in at least two distinct ethnic groups [Klopocki et al., 2008; Sun et al., 2008]. Sun et al. [2008] suggested that the smallest region of overlap (SRO) among various sizes of duplications in families they collected should be the critical region for PPD and SD4, which was strongly supported by our SD4 family. In comparison with seven other reported families with a duplication involving *ZRS* [Klopocki et al., 2008; Sun et al., 2008], the present family, even though with the smallest duplication, shows the most severe lower limb malforma-

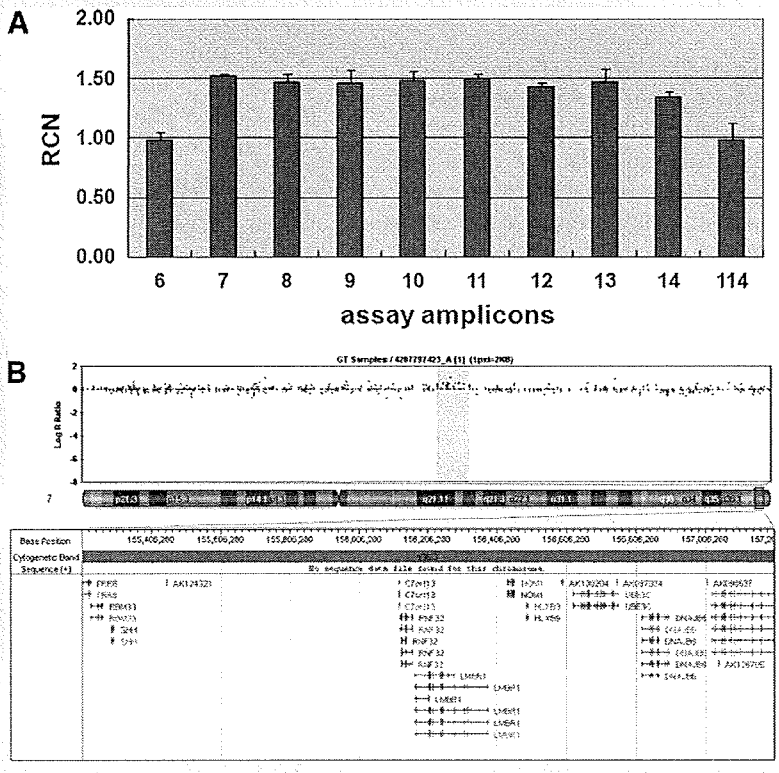

FIG. 1. Detection of *ZRS* duplication. A: The qPCR assay confirming a *ZRS* duplication in an affected individual (III-5). The duplication was seen as a 1.5-fold normalized RCN. B: Plots of the copy number for individual SNP loci along chromosome 7q by Illumina HumanHap550 Genotyping Chips, showing a 96,605 bp duplication from nt 156,240,230 to nt 156,336,835 at 7q36.3 in one affected member with tibial hypoplasia (IV-1). Schematic diagram of the known gene, *LMBR1*, affected by this duplication is depicted below the plots.

TABLE I. Clinical Phenotypes of 16 Reported Families With Mutations of *ZRS*

Mutations types	7 Point mutations	8 Duplications		
Clinical diagnosis, families [Refs.]	**PPD2/3, 8 [1–3]**	**SD4, 1 [4]**	**SD4-severe, 1 [5]**	**TPTPS, 6 [4, 6]**
Polydactyly				
Pre-axial	+	+	+	+
Post-axial	−	+	+	+
Hand	+	+	+	+
Foot	+	−	+	+
Mirror image	−	+	+	−
Triphalangeal thumb				
Single	+	−	−	+
Duplication	+	+	+	+
Syndactyly				
Complete	−	+	+	+
Partial	−	+	+	+
Cutaneous	−	+	+	+
Osseous	−	−	−	+
Hand	−	+	+	+
Foot	−	−	+	+
Cup-shaped hand	−	+	+	−
Tibial hypoplasia	−	−	+	−

1. Lettice et al. [2003]; 2. Gurnett et al. [2007]; 3. Furniss et al. [2008]; 4. Sun et al. [2008]; 5. Present study; 6. Klopocki et al. [2008].

tions. This may indicate that there is no correlation between phenotypic severity and the extent of duplications and in turn implies that a critical region for the disorders may exist within the smallest duplication. For detection of the copy number mutation, while the multiple qPCR assay used in the present study is rapid, sensitive and cheap, the SNP array method provides more precise results helpful for breakpoint mapping.

REFERENCES

Furniss D, Lettice LA, Taylor IB, Critchley PS, Giele H, Hill RE, Wilkie AO. 2008. A variant in the sonic hedgehog regulatory sequence (*ZRS*) is associated with triphalangeal thumb and deregulates expression in the developing limb. Hum Mol Genet 17:2417–2423.

Gillessen-Kaesbach G, Majewski F. 1991. Bilateral complete polysyndactyly (type IV Haas). Am J Med Genet 38:29–31.

Gurnett CA, Bowcock AM, Dietz FR, Morcuende JA, Murray JC, Dobbs MB. 2007. Two novel point mutations in the long-range *SHH* enhancer in three families with triphalangeal thumb and preaxial polydactyly. Am J Med Genet Part A 143A:27–32.

Haas SL. 1940. Bilateral complete syndactylism of all fingers. Am J Surg 50:363–366.

Heutink P, Zguricas J, van Oosterhout L, Breedveld GJ, Testers L, Sandkuijl LA, Snijders PJ, Weissenbach J, Lindhout D, Hovius SE, Oostra BA. 1994. The gene for triphalangeal thumb maps to the subtelomeric region of chromosome 7q. Nat Genet 6:287–292.

Kantaputra PN, Chalidapong P. 2000. Are triphalangeal thumb-polysyndactyly syndrome (TPTPS) and tibial hemimelia-polysyndactyly-triphalangeal thumb syndrome (THPTTS) identical? A father with TPTPS and his daughter with THPTTS in a Thai family. Am J Med Genet 93:126–131.

Klopocki E, Ott CE, Benatar N, Ullmann R, Mundlos S, Lehmann K. 2008. A microduplication of the long range *SHH* limb regulator (*ZRS*) is associated with triphalangeal thumb-polysyndactyly syndrome. J Med Genet 45:370–375.

Lettice LA, Horikoshi T, Heaney SJ, van Baren MJ, van der Linde HC, Breedveld GJ, Joosse M, Akarsu N, Oostra BA, Endo N, Shibata M, Suzuki M, Takahashi E, Shinka T, Nakahori Y, Ayusawa D, Nakabayashi K, Scherer SW, Heutink P, Hill RE, Noji S. 2002. Disruption of a long-range cis-acting regulator for *Shh* causes preaxial polydactyly. Proc Natl Acad Sci USA 99:7548–7553.

Lettice LA, Heaney SJ, Purdie LA, Li L, de Beer P, Oostra BA, Goode D, Elgar G, Hill RE, de Graaff E. 2003. A long-range *Shh* enhancer regulates expression in the developing limb and fin and is associated with preaxial polydactyly. Hum Mol Genet 12:1725–1735.

Rambaud-Cousson A, Dudin AA, Zuaiter AS, Thalji A. 1991. Syndactyly type IV/hexadactyly of feet associated with unilateral absence of the tibia. Am J Med Genet 40:144–145.

Sato D, Liang D, Wu L, Pan Q, Xia K, Dai H, Wang H, Nishimura G, Yoshiura K, Xia J, Niikawa N. 2007. A syndactyly type IV locus maps to 7q36. J Hum Genet 52:561–564.

Sun M, Ma F, Zeng X, Liu Q, Zhao XL, Wu FX, Wu GP, Zhang ZF, Gu B, Zhao YF, Tian SH, Lin B, Kong XY, Zhang XL, Yang W, Lo W, Zhang X. 2008. Triphalangeal thumb-polysyndactyly syndrome and syndactyly type IV are caused by genomic duplications involving the long-range, limb-specific *SHH* enhancer. J Med Genet 45:589–595.

Tsukurov O, Boehmer A, Flynn J, Nicolai JP, Hamel BCJ, Traill S, Zaleske D, Mankin HJ, Yeon H, Ho C, Tabin C, Seidman JG, Seidman C. 1994. A complex bilateral polysyndactyly disease locus maps to chromosome 7q36. Nat Genet 6:282–286.

Zguricas J, Heus H, Morales-Peralta E, Breedveld G, Kuyt B, Mumcu EF, Bakker W, Akarsu N, Kay SP, Hovius SE, Heredero-Baute L, Oostra BA, Heutink P. 1999. Clinical and genetic studies on 12 preaxial polydactyly families and refinement of the localisation of the gene responsible to a 1.9 cM region on chromosome 7q36. J Med Genet 36:32–40.

RESEARCH LETTER

AMERICAN JOURNAL OF
medical genetics

Prenatal Diagnosis of Costello Syndrome Using 3D Ultrasonography Amniocentesis Confirmation of the Rare HRAS Mutation G12D

Hideo Kuniba,[1,2]* Ritsuko K. Pooh,[3] Kensaku Sasaki,[4] Osamu Shimokawa,[4] Naoki Harada,[4] Tatsuro Kondoh,[2,5] Masanori Egashira,[2] Hiroyuki Moriuchi,[2] Koh-ichiro Yoshiura,[1] and Norio Niikawa[1,6]

[1]Department of Human Genetics, Nagasaki University Graduate School of Biomedical Sciences, Nagasaki, Japan

[2]Department of Pediatrics, Nagasaki University Graduate School of Biomedical Sciences, Nagasaki, Japan

[3]CRIFM Clinical Research Institute of Fetal Medicine PMC, Osaka, Japan

[4]Kyushu Medical Science Nagasaki Laboratory (KMS), Nagasaki, Japan

[5]Department of Clinical Genetics, Misakae-no-sono Mutsumi, Institute for Severe Intellectual/Motor Disabled Persons, Isahaya, Japan

[6]Research Institute of Personalized Health Sciences, Health Sciences University of Hokkaido, Tobetsu, Japan

Received 8 February 2008; Accepted 12 March 2008

TO THE EDITOR:

Costello syndrome (CS, OMIM #218040) is a rare disorder with a distinctive facial appearance, prenatal overgrowth, poor postnatal growth, loose skin of the hands and feet, characteristic hand position, developmental delay, papillomata, cardiac abnormalities, and tumor predisposition. *HRAS* is the only gene currently known to be causative for CS [Aoki et al., 2005; Nava et al., 2007; Rauen, 2007]. Almost all of the mutations of the *HRAS* gene in CS patients which have been reported subsequently have been diagnosed after infancy [Estep et al., 2006; Gripp et al., 2006; Kerr et al., 2006; Schulz et al., 2008] except for patients presenting with severe neonatal manifestation of CS [Lo et al., 2008]. We report on the first patient with prenatally diagnosed CS dues to the rare c.35G > A, p.G12D *HRAS* mutation.

A 31-year-old G2P1 woman was referred at 23 weeks of gestation for ultrasonography which showed polyhydramios, good fetal movement, and overgrowth with estimated body weight 1,300 g (+5.3 SD using a Japanese fetal growth curve). There was no pleural effusion, ascites or subcutaneous edema. Craniofacial features included large head (+3.0 SD), pointed chin, full cheeks, wide nasal bridge, and low-set ears (Fig. 1A), but no macroglossia, omphalocele, hydrocephalus, or brain anomalies. The size of the abdomen was equivalent to that of a fetus at 28–31 weeks gestation. The fetal stomach could not be identified. Hepatomegaly was detected, but the other visceral organs were normal. The extremities were normal in length without deformity, although the wrists were deviated laterally.

Cytogenetic and molecular analyses were performed after obtaining informed consent from parents. Standard chromosomes analysis by amniocentesis showed normal karyotype: 46,XY. The deletion of *NSD1* responsible for Sotos syndrome was not detected by fluorescence in situ hybridization (data not shown). By the time CS was suspected, the volume of amniotic fluid was only 1.8 ml which was frozen and stored in the clinic. To perform molecular diagnosis for CS, DNA was extracted with QIAvac vacuum manifold (Qiagen, Chatsworth, CA) from the specimen, and whole genome amplification was carried out with GenomePlex Whole Genome Amplification Kit (Sigma–Aldrich, St. Louis, MO), according to the manufacture's instructions. In this procedure, 3 μg of DNA was obtained. All *HRAS* coding exons and their flanking intronic sequences were analyzed by direct sequencing on an ABI 3100 automated sequencer (Applied Biosystems, Foster City, CA), and a rare missense mutation was found, that is, c.35G > A, p.G12D (Fig. 1B).

How to Cite this Article:
Kuniba H, Pooh RK, Sasaki K, Shimokawa O, Harada N, Kondoh T, Egashira M, Moriuchi H, Yoshiura K, Niikawa N. 2009. Prenatal diagnosis of Costello syndrome using 3D ultrasonography amniocentesis confirmation of the rare HRAS mutation G12D.
Am J Med Genet Part A 149A:785–787.

*Correspondence to:
Dr. Hideo Kuniba, Department of Pediatrics, Nagasaki University Graduate School of Biomedical Sciences, Sakamoto 1-12-4, Nagasaki 852-8523, Japan. E-mail: kuniba03@nifty.com

Published online 18 July 2008 in Wiley InterScience (www.interscience.wiley.com)
DOI 10.1002/ajmg.a.32335

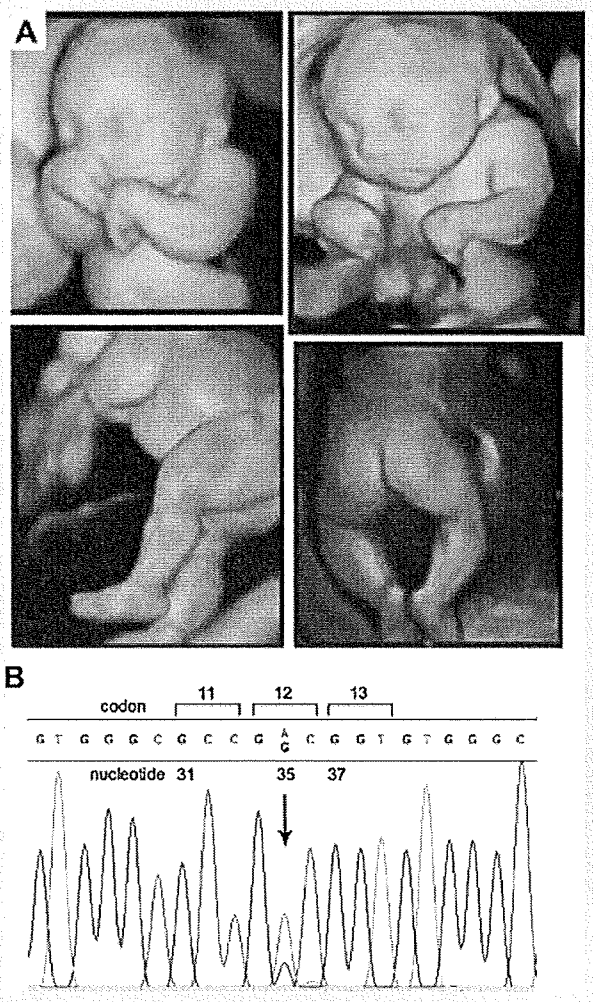

FIG. 1. A: Three-dimensional ultrasound images of the fetus at 24 weeks of gestation with overgrowth and so-called "coarse face". Note his left hand presenting ulnar deviation and flexion of the wrist. B: Electropherogram of *HRAS* showing missense mutation at codon 12, c.35G > A, p.G12D. [Color figure can be viewed in the online issue, which is available at www.interscience.wiley.com.]

The mother had been transported to a pediatric hospital after the fetal evaluation, and the fetus subsequently developed pleural effusion and deteriorated. He was born at 31 weeks gestation via cesarean. He weighed 2,926 g (+4.2 SD) and developed respiratory failure, severe hypoglycemia, cardiac hypertrophy and renal failure. Although he was treated in neonatal intensive care unit, he died soon after birth due to multiple organ failures. Permission for autopsy was not granted. We were unable to study the parental origin [Sol-Church et al., 2006; Zampino et al., 2007] because DNA samples from the mother and his 33-year-old father had not been obtained.

Prenatal overgrowth and polyhydramios were prominent in this case. Dysmorphic facial features and flexion of the wrist, imaged with striking clarity by three-dimensional (3D) ultrasonography led us to a clinical diagnosis of CS. Prenatal overgrowth syndromes include relatively few conditions, that is, Sotos syndrome, Simpson–Golabi–Behmel syndrome, Beckwith–Wiedemann syndrome, and CS. The presence of polyhydramios which occurs in over 90% of pregnancies with CS, supported by the 3D ultrasonographic imaging of facial features (broad nose, puffy cheeks, so-called "coarse" face, pointed chin, and flexion of the wrist) made the diagnosis likely. Three-dimensional ultrasonography is clearly more beneficial than two-dimensional (2D) ultrasonography in a diagnosis of genetic syndromes, since we can see overall fetal image of malformation which we hardly get with conventional 2D ultrasonography [Lee and Simpson, 2007]. The phenotype of Noonan syndrome often overlaps with that of CS, and the prenatal findings of Noonan syndrome, polyhydramnios and so-called "coarse face" in a fetus with the T854C mutation in the *PTPN11* gene, have been reported [Levaillant et al., 2006], although that fetus with Noonan syndrome did not develop overgrowth.

CS was diagnosed clinically in the prenatal period in monozygotic twins who died 57 days of life after birth at 30 weeks of gestation due to respiratory failure [Van den Bosch et al., 2002]. Molecular diagnosis was not available. Neonatal deaths in two patients with CS confirmed by molecular diagnosis of G12D *HRAS* mutation were reported by Lo et al. [2008]. One patient was born at 36 weeks gestation weighing 2,950 g developed hypoglycemia, persistent and severe jaundice, persistent respiratory distress with tracheomalacia, bronchomalacia and chylothorax. The baby also had clenched hands, atrial septal defect, paroxysmal multifocal atrial tachycardia, pulmonary lymphangiectasia, and renal failure. She died at age 3 months due to respiratory failure. The other patient was a girl born at 37 weeks gestation weighing 3,115 g had hypoglycemia, rhizomelic limb shortening and flexion contractures at the wrist, hypertrophic cardiomyopathy, dysplasic pulmonary valve, atrial fibrillation, cardiac failure and persistent hyponatremia due to renal sodium leakage. She became ventilator dependent and died at 3 months of age from sepsis and renal failure. Both had pregnancies complicated by polyhydramios. Lo et al. [2008] suggested that differences in activating potential of G12D mutations in *HRAS* gene may result in severe manifestations, such as hypoglycemia, renal abnormalities, severe early cardiomyopathy, and congenital respiratory abnormalities, which result in multiple organ failure.

We believe this is the first case of prenatally diagnosed CS confirmed with molecular genetic analysis with a G12D mutation in *HRAS* gene. The mutation was not observed in previous natural history studies of CS, perhaps because of the rarity of the mutation and the fact that the patients die in early infancy. Our findings contribute to the natural history of this mutation which includes a severe clinical course. If prenatal ultrasonographic findings show both polyhydramnios and overgrowth, CS should be considered despite its rarity. Molecular diagnosis should be offered in the perinatal period without hesitation.

ACKNOWLEDGMENTS

We are grateful to the family for their participation in this research. We thank Dr. Shoko Miura for her helpful comments.

REFERENCES

Aoki Y, Niihori T, Kawame H, Kurosawa K, Ohashi H, Tanaka Y, Filocamo M, Kato K, Suzuki Y, Kure S, Matsubara Y. 2005. Germline mutations in HRAS proto-oncogene cause Costello syndrome. Nat Genet 37: 1038–1040.

Estep AL, Tidyman WE, Teitell MA, Cotter PD, Rauen KA. 2006. HRAS mutations in Costello syndrome: Detection of constitutional activating mutations in codon 12 and 13 and loss of wild-type allele in malignancy. Am J Med Genet Part A 140A:8–16.

Gripp KW, Lin AE, Stabley DL, Nicholson L, Scott CI Jr, Doyle D, Aoki Y, Matsubara Y, Zackai EH, Lapunzina P, Gonzalez-Meneses A, Holbrook J, Agresta CA, Gonzalez IL, Sol-Church K. 2006. HRAS mutation analysis in Costello syndrome: Genotype and phenotype correlation. Am J Med Genet Part A 140A:1–7.

Kerr B, Delrue MA, Sigaudy S, Perveen R, Marche M, Burgelin I, Stef M, Tang B, Eden OB, O'Sullivan J, De Sandre-Giovannoli A, Reardon W, Brewer C, Bennett C, Quarell O, M'Cann E, Donnai D, Stewart F, Hennekam R, Cave H, Verloes A, Philip N, Lacombe D, Levy N, Arveiler B, Black G. 2006. Genotype-phenotype correlation in Costello syndrome: HRAS mutation analysis in 43 cases. J Med Genet 43:401–405.

Lee YM, Simpson LL. 2007. Major fetal structural malformations: The role of new imaging modalities. Am J Med Genet Part C Semin Med Genet 145C:33–44.

Levaillant JM, Gerard-Blanluet M, Holder-Espinasse M, Valat-Rigot AS, Devisme L, Cave H, Manouvrier-Hanu S. 2006. Prenatal phenotypic overlap of Costello syndrome and severe Noonan syndrome by tridimensional ultrasonography. Prenat Diagn 26:340–344.

Lo IF, Brewer C, Shannon N, Shorto J, Tang B, Black G, Soo MT, Ng D, Lam ST, Kerr B. 2008. Severe neonatal manifestations of Costello syndrome. J Med Genet 45:167–171.

Nava C, Hanna N, Michot C, Pereira S, Pouvreau N, Niihori T, Aoki Y, Matsubara Y, Arveiler B, Lacombe D, Pasmant E, Parfait B, Baumann C, Héron D, Sigaudy S, Toutain A, Rio M, Goldenberg A, Leheup B, Verloes A, Cavé H. 2007. Cardio-facio-cutaneous and Noonan syndromes due to mutations in the RAS/MAPK signalling pathway: Genotype-phenotype relationships and overlap with Costello syndrome. J Med Genet 44:763–771.

Rauen KA. 2007. HRAS and the Costello syndrome. Clin Genet 71: 101–108.

Schulz AL, Albrecht B, Arici C, van der Burgt I, Buske A, Gillessen-Kaesbach G, Heller R, Horn D, Hübner CA, Korenke GC, König R, Kress W, Krüger G, Meinecke P, Mücke J, Plecko B, Rossier E, Schinzel A, Schulze A, Seemanova E, Seidel H, Spranger S, Tuysuz B, Uhrig S, Wieczorek D, Kutsche K, Zenker M. 2008. Mutation and phenotypic spectrum in patients with cardio-facio-cutaneous and Costello syndrome. Clin Genet 73:62–70.

Sol-Church K, Stabley DL, Nicholson L, Gonzalez IL, Gripp KW. 2006. Paternal bias in parental origin of HRAS mutations in Costello syndrome. Hum Mutat 27:736–741.

Van den Bosch T, Van Schoubroeck D, Fryns JP, Naulaers G, Inion AM, Devriendt K. 2002. Prenatal findings in a monozygotic twin pregnancy with Costello syndrome. Prenat Diagn 22:415–417.

Zampino G, Pantaleoni F, Carta C, Cobellis G, Vasta I, Neri C, Pogna EA, De Feo E, Delogu A, Sarkozy A, Atzeri F, Selicorni A, Rauen KA, Cytrynbaum CS, Weksberg R, Dallapiccola B, Ballabio A, Gelb BD, Neri G, Tartaglia M. 2007. Diversity, parental germline origin, and phenotypic spectrum of de novo HRAS missense changes in Costello syndrome. Hum Mutat 28:265–272.

Gene 432 (2009) 97–101

Contents lists available at ScienceDirect

Gene

journal homepage: www.elsevier.com/locate/gene

Developmentally dynamic changes of DNA methylation in the mouse *Snurf/Snrpn* gene

Kazumi Miyazaki [a], Christophe K. Mapendano [b], Tomokazu Fuchigami [c], Shinji Kondo [a], Tohru Ohta [d], Akira Kinoshita [b], Kazuhiro Tsukamoto [c], Ko-ichiro Yoshiura [b], Norio Niikawa [b], Tatsuya Kishino [a,*]

[a] *Division of Functional Genomics, Center for Frontier Life Sciences, Nagasaki University, Sakamoto 1-12-4, Nagasaki 852-8523, Japan*
[b] *Department of Human Genetics, Graduate School of Biomedical Sciences, Nagasaki University, Nagasaki, 852-8523, Japan*
[c] *Department of Pharmacotherapeutics, Graduate School of Biomedical Sciences, Nagasaki University, Nagasaki, 852-8523, Japan*
[d] *Research Institute of Personalized Health Sciences, Health Sciences University of Hokkaido, Hokkaido, 061-0293, Japan*

ARTICLE INFO

Article history:
Received 29 August 2008
Received in revised form 9 November 2008
Accepted 16 November 2008
Available online 27 November 2008

Received by T. Sekiya

Keywords:
Imprinting
Snrpn
DNA methylation
DMR
Enhancer

ABSTRACT

The mouse *Snurf/Snrpn* gene has two differentially methylated regions (DMRs), the maternally methylated region at the 5′ end (DMR1) and the paternally methylated region at the 3′ end (DMR2). DMR1, a region that includes the *Snrpn* promoter and the entire intron 1, has been thought to be a germline DMR, which inherits the parental-specific methylation profile from the gametes. DMR1 is not only associated with imprinted *Snrpn* expression, but implicated in imprinting control of other genes in the region. We have now characterized the highly conserved activator sequence (CAS) in the *Snrpn* intron 1 among human and rodents and demonstrate that the mouse CAS is not a germline DMR but shows developmentally dynamic changes of DNA methylation and has methylation-sensitive enhancer activity. The tissue-specific methylation of the mouse CAS and its methylation-sensitive enhancer activity may control tissue-specific expression of IC transcripts, resulting in the establishment and/or maintenance of imprinting in the *Snrpn* locus.

1. Introduction

Genomic imprinting is an important mechanism of gene regulation, which causes genetic nonequivalence in expression between maternal and paternal genomes in mammals. Such parent-of-origin specific gene regulation is caused by epigenetic modifications, which initially occur during gametogenesis without any nucleic acids changes (Surani, 1998; Tilghman, 1999). Epigenetic modifications in gametes continue to differentiate alleles of parental origin even after zygote formation, so that one parentally-derived allele eventually becomes preferentially expressed. One of the epigenetic modifications in imprinting is DNA methylation. DNA methylation can be stably inherited in somatic cells and reset in gametes. In the imprinted loci, differentially methylated regions (DMRs) between the maternal and paternal alleles are often found and associated with parent-allele-specific expression. For some imprinted loci, DMRs are gamete-derived methylated regions (germline DMRs), where DNA methylation in the gamete is maintained throughout development in all somatic lineages. However, there exist secondary DMRs, which are acquired during development and associated with primary imprints in the gamete (Constancia et al. 1998). Although the primary DMRs are essential for establishment and maintenance of imprinting, which are associated with the imprinting center (IC) (Bourc'his et al. 2001; Hata et al. 2002), it is unknown whether the secondary DMRs directly control the imprinted expression or exist only as the consequence of an epigenetic event.

The mouse chromosome 7C is a large imprinted domain orthologous to the Prader-Willi syndrome (PWS)/Angelman syndrome (AS) critical region at human chromosome 15q11-q13. The imprinted domain 7C contains paternally expressed genes, *Snurf/Snrpn* (hereafter termed *Snrpn*), *Ndn*, *Magel2*, *Mkrn3* and C/D-box small nucleolar RNAs (snoRNAs), and the maternally expressed gene, *Ube3a* (Nicholls and Knepper, 2001). Imprinted expression within this large domain is coordinated by a bipartite cis-acting IC located upstream from the *Snrpn* gene. In the large imprinted domain, several DMRs have been identified. One of them is in the *Snrpn* locus, which has two DMRs (Fig. 1A), the 5′ end methylated on the maternal allele (DMR1) and the 3′ end methylated on the paternal allele (DMR2) (Shemer et al. 1997; Gabriel et al. 1998). DMR1 is a ~6 kb region containing the 5′ end of the *Snrpn* gene and the entire *Snrpn* intron 1 (Fig. 1A). DMR2 is a 3.5-kb region spanning exons 7–10. Both DMR1 and DMR2 are thought as germline DMRs, which inherit the parental-specific methylation profile from the

Abbreviations: AS, Angelman syndrome; CAS, conserved activator sequence; ChIP, Chromatin immunoprecipitation; DHS, nuclease hypersensitive sites; DMR, differentially methylated region; IC, imprinting center; PWS, Prader-Willi syndrome; SMP, *Snrpn* minimal promoter; UPD, uniparental disomy.

* Corresponding author. Fax: +81 95 819 7178.
E-mail address: kishino@nagasaki-u.ac.jp (T. Kishino).

0378-1119/$ – see front matter © 2008 Elsevier B.V. All rights reserved.
doi: 10.1016/j.gene.2008.11.019

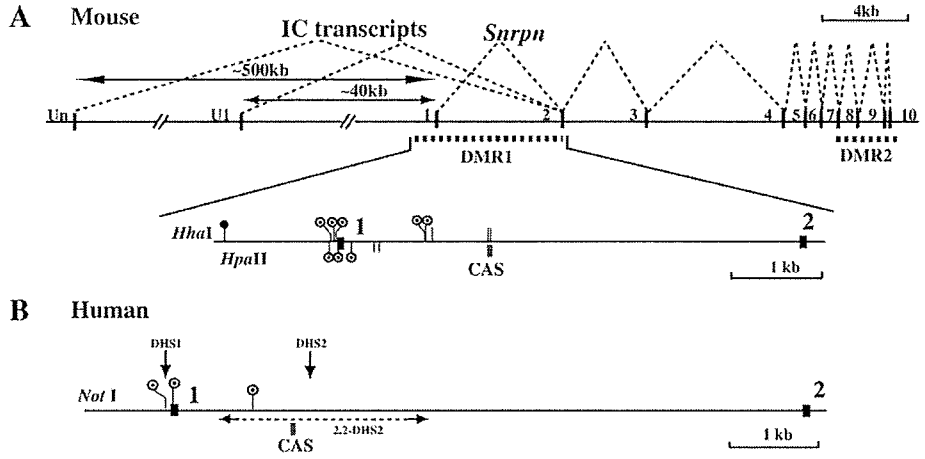

Fig. 1. Genomic organization and the DNA methylation pattern of the mouse (A) and human (B) *Snrpn/SNRPN* locus. Black and gray boxes indicate exons and the CAS region. (A) IC transcripts overlap with *Snrpn* except exon 1. Spliced exons except U exons in IC transcripts are omitted. Short vertical lines above and below the horizontal line indicate 8 *Hha*I and 5 *Hpa*II sites in DMR1, respectively (GenBank accession. no. AC167813). (B) Short vertical lines above the horizontal line indicate 3 *Not*I sites in DMR1. Solid and dotted circles indicate biallelically methylated sites and maternal allele-specific methylated sites (Shemer et al. 1997; Lucifero et al. 2002; Glenn et al. 1996). The *Bss*HII site is described as two *Hha*I sites with dotted circles.

gamete (Shemer et al. 1997). Since DMR1 contains the IC, the methylation status of DMR1 is not only associated with paternal-allele-specific expression of *Snrpn* but may be implicated in imprinting control of other genes in the region.

In the human *SNRPN* locus, parental origin-specific nuclease hypersensitive sites (DHSs) have been identified (Schweizer et al. 1999; Rodriguez-Jato et al. 2005). One of the paternal origin-specific DHSs is DHS1 in the *SNRPN* promoter and the other is DHS2 in *SNRPN* intron 1, roughly 1.5 kb downstream of the transcription initiation site (Fig. 1B). Differential methylation of the CpG island flanking DHS1 is well characterized as a maternal allele-specific DMR in the *SNRPN* promoter. The CpG island associated with DHS2 was reported to show maternal allele-specific methylation in lymphoblastoid cell lines (Rodriguez-Jato et al. 2005), and to be distinct and separate from the CpG rich region in intron 1, 0.9 kb downstream of the transcription initiation site, which was previously described as a DMR in fetal tissues (Fig. 1B) (Glenn et al. 1996). Interestingly, an intronic 2.2-kb fragment (2.2-DHS2) associated with DHS2 was found to enhance the activity of the *SNRPN* promoters (Rodriguez-Jato et al. 2005). The especially highly conserved sequence (CAS) in 2.2-DHS2 among human and rodent was identified to have enhancer activity in human (Fig. 1B). Chromatin immunoprecipitation (ChIP) analysis revealed that the CAS showed paternal chromatin-specific interaction with transcription factors (Rodriguez-Jato et al. 2005). These data suggest that the CAS may play a critical role in activating the paternally expressed imprinted genes in the domain. It remains unknown whether such an allele-specific interaction with transcription factors depends on allele-specific DNA methylation in the CAS and how imprinted transcripts in the *SNRPN* locus can be controlled by the enhancer activity of the CAS.

To investigate further functions of the CAS in the imprinting domain, we analyzed the methylation status of the mouse CAS and a methylation effect on the enhancer activity of the CAS. Our results show that the *Snrpn* promoter region in DMR1 is a germline DMR as previously reported (Shemer et al. 1997), whereas the mouse CAS is a secondary DMR, which is acquired in a tissue-specific manner during development and has the methylation-sensitive activator function.

2. Materials and methods

2.1. Tissues and cells used

All procedures in mice were performed with approval from the Nagasaki University Institutional Animal Care and Use Committee. F1 hybrid mice were obtained by mating C57BL/6 females with PWK males (C57BL/6×PWK), and vice versa (PWK×C57BL/6). Methods of primary cultures of cortical neurons, glial cells and embryonic fibroblasts were described elsewhere (Yamasaki et al. 2005). Oocytes and sperm collections were performed as described elsewhere (Mapendano et al. 2006; Yoshida et al. 1995).

2.2. DNA extraction from gametes, cells and tissues

To prepare oocyte DNA, about 400 pooled oocytes were resuspended in 160 μL of 10 mM Tris–HCl (pH 8.0), 10 mM EDTA, 150 mM NaCl, 0.1% SDS, 2 μg of λ DNA, and 40 μg of proteinase K and incubated for 3 h at 55°C, then extracted with phenol-chloroform and precipitated with ethanol. Blastocyst DNA was prepared from about 10–15 blastocysts with the same procedure. Sperm DNA was isolated by the two-digestion method as described (Yoshida et al. 1995). DNA from other embryos, tissues and human blood was extracted as described elsewhere (Yamasaki et al. 2005).

2.3. Sodium bisulfite treatment and sequencing

Sodium bisulfite treatment was carried out using EZ DNA Methylation-Gold kit (Zymo Research. Orange, CA). PCRs were carried out using bisulfite-treated DNA and each primer set. The following primer pairs were used for amplification: Snrpn-outsideF/Snrpn-outsideR for DMR1 (Lucifero et al. 2002); mCAS-F/mCAS-R for the mouse CAS; hCAS-F/hCAS-R for the human CAS. Primer sequences are as follows: mCAS-F 5′-TGGGGAGGGGTTTATTGTTTTG-3′; mCAS-R 5′-ATAACATCCTAAATTTTAT CAAAATCAT-3′; hCAS-F 5′-TTGGGAAT-TAGGTTTTGGAAGGTT-3′; hCAS-R 5′-ACCTACCCCCTCCCCACTAAC-3′. The amplification protocol was as follows: denaturation at 94 °C for 6 min, followed by 40 cycles at 94 °C for 1 min, 55 °C for 2 min, 72 °C for 2 min, and final elongation at 72 °C for 10 min. PCR products were ligated into PCR2.1 vector by TOPO TA Cloning Kit (Invitrogen, Carlsbad, CA) and sequenced on ABI PRISM Model3100.

2.4. Reporter gene construction, methylation, and reporter gene transfection assay

The *Snrpn* promoter regions and the CAS were amplified with following primers: SnrpnL-F/SnrpnL-R for the *Snrpn* promoter; SMP-F/SMP-R for the SMP; U1-F/U1-R for the U1 promoter; mCASL-F/mCASL-R for the CAS. Primer sequences are as follows. SnrpnL-F 5′-

AAGCCCTGTCTCTAAAACCAAC-3′, SnrpnL-R 5′-CTTCCTCGCTCCATTGC-GTTG-3′, SMP-F 5′-CGAGCTCAAATGTGCGCATGTGCAGCC-3′, SMP-R 5′-GCTCGAGCTTCCTCGCTCCATTGCGTTG-3′, U1-F 5′-CGAGCTCATT-CATCACAATGAAAATCAATA-3′, U1-R 5′-CCGCTCGAGCTTGGTTGCTG-CATTGCCTTG-3′, mCASL-F 5′-AGATCTAAGGGGTCGTGTCGCATGTC-3′, mCASL-R 5′-AGATCTGTATACGCCATGCTGCGCC-3′.

PCR products were directly ligated into PCR2.1 vector by TOPO TA Cloning Kit, followed by *Sac*I /*Xho*I double digestion for the *Snrpn* promoter, SMP and the U1 promoter, and by *Bgl*II digestion for the CAS. The *Sac*I/*Xho*I digested products were cloned into the *Sac*I/*Xho*I sites upstream of the firefly luciferase gene and the *Bgl*II digested product was into the *Bam*HI site downstream of the firefly luciferase gene of pGL4.10 (Promega, Madison, WI). *In vitro* methylation of the constructs, plasmids (10 μg) were incubated for 1 h at 37°C in the presence or absence (control, mock) of *Hha*I and *Sss*I methylase (New England BioLabs, Beverly, MA). Plasmids were transfected into Neuro2a cells, using Lipofectamine 2000 reagent (Invitrogen). The pGL4.70, encoding the renilla luciferase gene (Promega) was cotransfected as an internal control for transfection efficiency. Transfected cells were harvested after 24 h and used for measuring firefly and renilla luciferase activities in Dual-Luciferase Assay system (Promega). Reporter activity was normalized by calculating the ratio of firefly to renilla values. For each construct, the average and standard error of the means were calculated in 6 independent transfections.

3. Results and discussion

3.1. The mouse CAS shows developmental stage-specific methylation and maternal allele-specific methylation in the brain

It has been confirmed by many experiments that maternal allele-specific DNA methylation of the *Snrpn* promoter region in DMR1 originates from the egg and is maintained throughout development (Shemer et al. 1997). However, the methylation pattern of the *Snrpn* intron 1 in DMR1 has not been precisely analyzed except in several recognition sites of methylation-sensitive restriction enzymes, *Bss*HII and *Hha*I (Fig. 1A) (Shemer et al. 1997; Gabriel et al. 1998). We first performed methylation analysis of the *Snrpn* promoter region and the mouse CAS in the *Snrpn* intron 1, which is located ~1.8 kb downstream of the *Snrpn* transcription initiation site. Parental origin of the alleles was identified by polymorphic sites in F1 hybrids between C57BL/6 and PWK strains (divergent strains of *Mus musculus*). Allele-specific methylation of 16 CpGs in the promoter and 7 CpGs in the CAS was examined using polymorphisms in PCR products of bisulfite-modified DNA. Sequencing of clones from the PCR products revealed maternal allele-specific methylation of the promoter region in the gametes and somatic tissues (data not shown) as previously reported (Shemer et al. 1997), whereas the CAS showed a different methylation pattern depending on tissues (Fig. 2). In oocytes and sperm, all 7 CpGs in the CAS were not methylated (Fig. 2A). In blastocysts, the maternal allele was slightly methylated, and completely methylated in the whole embryo at embryonic day (E) 9.5. In contrast, the paternal allele was not methylated in blastocysts and the whole embryos at E9.5, and moderately methylated in the embryonic liver and muscle at E15. In the embryonic brain, the paternal allele was almost unmethylated. In the adult brain, the CAS was not methylated on the paternal allele, while in the adult liver, muscle, kidney, and blood, they were biallelically methylated (Fig. 2B). These data indicate that the CAS is a secondary DMR, which is acquired in a tissue-specific manner during development. These results do not conflict with the previous methylation profile of DMR1, reported by Shemer et al. (1997). They detected differential methylation of the *Hha*I site in the CAS in ES cells and brains. In their Southern blot, the CAS is exclusively unmethylated in androgenetic ES cells, while in the parthenogenetic ES cells, the CAS is not completely methylated, although they concluded the maternal allele-specific methylation. The reason why the CAS in parthenogenetic ES cells showed almost methylated might be that the maternal

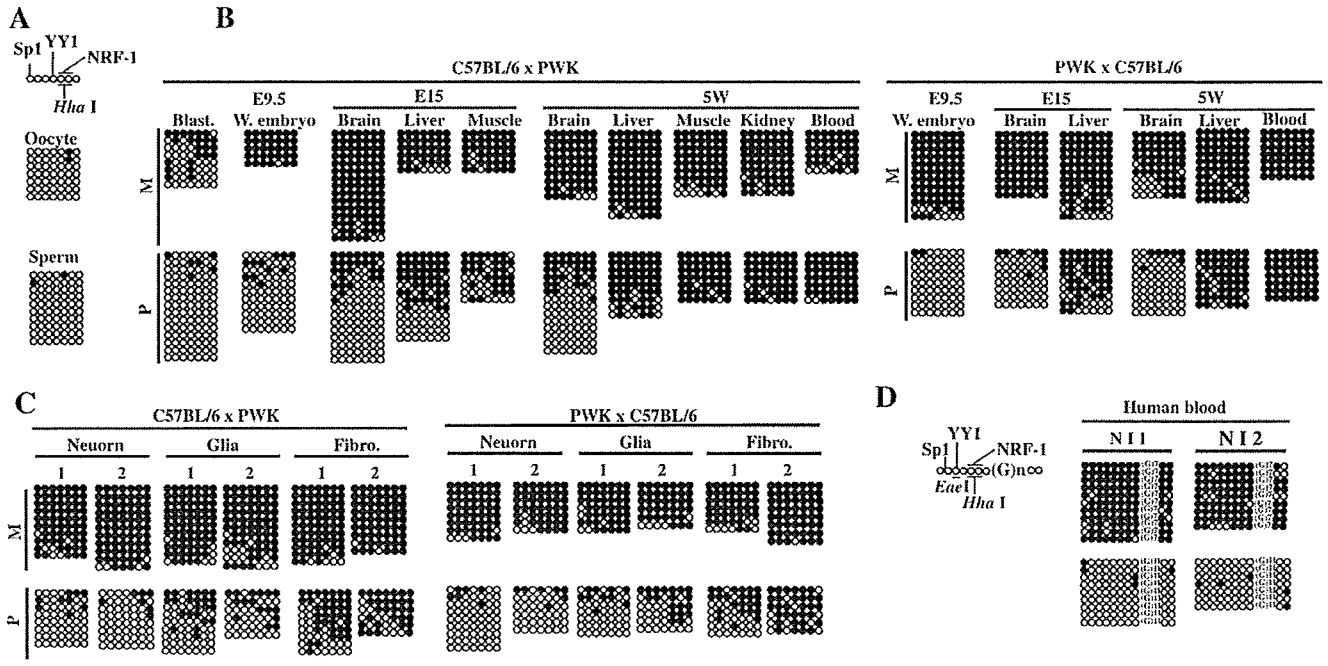

Fig. 2. Methylation of CpG dinucleotides in the CAS in gametes, tissues and culture cells in mice (A, B, C) and in human lymphocytes (D). Each row of dots represents the series of CpGs in an individual sequence molecule, in which methylated CpGs are shown as solid circles and unmethylated CpG as open circles. (A) Mouse oocytes and sperm. The properties of the mouse CAS are displayed at the top of the figure. (B) Embryonic and adult tissues of F1 hybrid mice. Blast.: Blastocyst, W.embryo: Whole embryo, M: maternal allele, P: paternal allele. (C) Culture cells. Two independent sets (1, 2) of each type of culture cells were used for methylation analysis in the CAS. Fibro. : embryonic fibroblasts. (D) Human peripheral bood from normal individuals (NI1 and NI2). The properties of the human CAS are displayed at the left of the figure.

allele in the CAS tends to rapidly acquire DNA methylation after the genome-wide demethylation, even if the parthenogenetic ES cells keep their multipotency during *in vitro* culture.

3.2. Allele-specific methylation of the mouse CAS is not neuron-specific in culture cells

In the embryonic and adult brains, most clones from the paternal alleles at the mouse CAS were not methylated but small numbers of clones were methylated, especially in the F1 hybrid (C57BL/6×PWK) brain. To know the cell origin of the methylated clones, we analyzed the methylation status in cultured neurons, glial cells and embryonic fibroblasts, which were separately cultured from embryonic tissues at E15.5 (Yamasaki et al. 2005). Prior to the analysis, we confirmed by immunostaining with the brain precursor, neuronal and glial makers that over 95% of the two cultured cell types were postmitotic neurons and astrocytes, respectively (data not shown). In neurons and glial cells, most clones from the paternal allele were not methylated, but more methylated clones were detected in glial cells than in neurons, while in the embryonic fibroblasts, many but not all of the paternal clones were methylated (Fig. 2C). We could not detect distinct differences in the methylation profile between cultured neurons and glial cells, as we previously reported in *Igf2r* DMR2 (Yamasaki et al. 2005). Although we could not completely deny the possibility that the tissue-specific methylation profile might not be stably established during *in vitro* differentiation in the embryonic cell culture, these data suggest that the paternal allele escapes methylation during neurogenesis and gliogenesis.

3.3. The human CAS shows allele-specific methylation in the normal lymphocyte

The methylation pattern of the human CAS has previously been reported using genomic DNA from the cell lines derived from uniparental disomy (UPD) patients of PWS and AS (Rodriguez-Jato et al. 2005). Because our bisulfite methylation analysis revealed that the CAS is biallelically methylated in most adult tissues including the lymphocytes in mice, we tried to confirm the methylation status of the human CAS in the normal lymphocyte. A G-nucleotide number polymorphism (Gn; $n=7,11$) was used to differentiate parental alleles in two normal individuals. We could not identify the parental origin of the alleles because no parental DNA was available, however, the human CAS showed allele-specific methylation in the human peripheral blood lymphocyte (Fig. 2D). We also examined allele-specific methylation in tissues of seven fetuses, but failed to prove it because we could not find any polymorphic sites flanking the CAS in the samples. Although based on a limited number of samples, our data about allele-specific methylation in the normal lymphocyte, in addition to the previous report about the maternal allele-specific methylation in the cell line of UPD patients, strongly suggests that the human CAS is a DMR in differentiated tissues.

3.4. The mouse CAS has a methylation-sensitive activator function

The human CAS was reported not only to activate the *SNRPN* promoter, but also the heterologous promoters in transient expression assays (Rodriguez-Jato et al. 2005). To see if the mouse CAS also has such a promoter activating function, transient expression assays were performed in mouse neuroblastoma Neuro2a cells (Fig. 3). The entire 80 bp of the mouse CAS was inserted to luciferase reporter constructs that include a 754-bp segment of the *Snrpn* promoter (from positions −679 to +75) or a 159-bp segment of the *Snrpn* minimal promoter (SMP) (from positions −84 to +75) (Hershko et al. 1999). Constructs in which the mouse CAS was cloned downstream from the mouse *Snrpn* promoter or the SMP showed approximately 3.5-fold increase in reporter activity, compared with control constructs lacking the mouse CAS. Similar results were obtained independent of orientation and position of the CAS in Neuro2a (data not shown).

Since the mouse CAS shows the tissue-specific and developmental stage-specific methylation, an effect of methylation on the promoter activation function was examined. The methylation effect on two *Hhal* sites in the mouse CAS was analyzed in the constructs with the *Snrpn* upstream promoter U1 (Fig. 1A), because the U1 promoter sequence has no *Hhal* sites. The U1 promoter region was cloned into a luciferase reporter construct that included the CAS positioned downstream of the reporter in the forward orientation. Transient expression assays revealed that the U1 promoter was activated by the CAS relative to a construct lacking the CAS (5.5 fold). *In vitro* methylation by *Hhal* methylase prior to transfection of Neuro2a cells activated the U1 promoter activity to a less extent (2 fold) than no methylation in the CAS. *In vitro* methylation of the five CpGs within the U1 promoter and seven CpGs within the CAS by *Sssl* methylase resulted in a complete

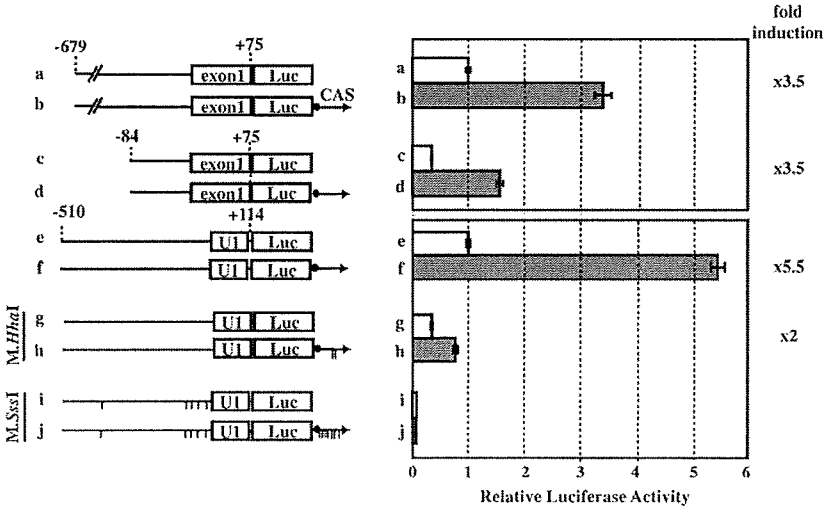

Fig. 3. Methylation-sensitive enhancer activity of the mouse CAS. Reporter constructs with the *Snrpn* promoter (a, b), the *Snrpn* minimal promoter (c, d), and the U1 promoter (e, f, g, h, i, j) lacking or carrying the mouse CAS (arrow) were assayed by transient expression assays. In the constructs (g, h, i, j), *in vitro* methylation with *Hhal* (g, h) or *Sssl* (i, j) methylases was performed. Short vertical lines below the lines and arrows (h, i, j) indicate methylated CpGs. The constructs containing the *Snrpn* promoters (a), or the U1 promoter (e) without the CAS are arbitrarily assigned the value 1. The fold increase induced by the CAS or *in vitro* methylated CAS is indicated on the right.

shut-off of the promoter activity. These data indicate that the mouse CAS has the promoter activation function and its activity depends partially on the methylation status of the *Hha*I sites in the CAS.

In the human and rodent CAS, potential binding sites for transcription factors Sp1, YY1, and NRF-1 are highly conserved (Rodriguez-Jato et al. 2005). It is reasonable in our study that methylation of the two *Hha*I sites at the NRF-1 binding sequence directly decreased the enhancer activity because of methylation-sensitive binding of NRF-1 (Smith et al. 2004), however the fact that the CAS with methylated NRF-1 binding site still have enhancer activity suggests other factors including Sp1 and YY1 may coordinately constitute the enhancer complex at the paternal CAS.

In addition to the methylation-sensitive enhancer activity, the evidence that the mouse CAS is not methylated in oocytes and not methylated on the paternal allele in the brain, correlates with tissue-specific expression of IC transcripts, which initiate in U exons (Un) that are distributed in a 500-kb region upstream of *Snrpn* and overlap with *Snrpn* exons except exon 1 (Fig. 1A). In mice, IC transcripts are exclusively expressed in the ovary and brain, especially in oocytes and neurons (Mapendano et al. 2006), where the CAS is unmethylated and differentially methylated, respectively (Fig. 2A, C). The function of IC transcripts remains unknown, but the tissue-specific methylation of the mouse CAS and its methylation-sensitive enhancer activity may control tissue-specific expression of IC transcripts, resulting in the establishment of imprinting in oocytes (Mapendano et al. 2006) and neuron-specific imprinting of *Ube3a* in the brain, possibly by the antisense *Ube3a* transcript as a part of IC transcripts.

On the other hand, in human, there is no simple correlation of expression level of the IC transcripts and the CAS methylation. IC transcripts are expressed in some tissues including adult heart, brain, and ovary, but not in blood (Dittrich et al.1996), where the CAS is differentially methylated (Fig. 2D) and associated with allele-specific histone modifications and interactions with multiple regulatory proteins (Rodriguez-Jato et al. 2005). Such difference in DNA methylation in the CAS and expression of IC transcripts between human and mouse may support divergency of imprinting mechanism among species (Johnstone et al. 2006). The targeted replacement of the mouse PWS-IC with the equivalent human region in mice failed to maintain methylation on the maternal allele in somatic tissues and to protect the upstream genes (*Ndn* and *Mkrn3*) during *de novo* methylation in early embryogenesis (Johnstone et al. 2006). They suggested that the factors responsible for postzygotic maintenance of the imprint have diverged between human and mouse. Because their targeted PWS-IC region contains the CAS, where methylation is postzygotically acquired in mice, methylation status of the substituted CAS might be altered in oocyte and/or in early embryogenesis, resulting in failure of maintenance of imprinting. It is still controversial in human whether the methylation imprint at the *SNRPN* promoter region is established in ovulated oocyte or during/following fertilization (El-Maarri et al. 2001; Geuns et al. 2003), however the timing of DNA methylation acquisition at the substituted CAS in the targeted mouse will clarify the basic difference in imprinting machinery among human and rodents.

In conclusion, we have demonstrated that the *Snrpn* intron 1, which was previously thought to be a part of a germline DMR in mouse, shows developmentally dynamic changes of DNA methylation in mouse, and has the methylation-sensitive enhancer activity. The tissue-specific methylation of the mouse CAS and its methylation-sensitive enhancer activity may control tissue-specific expression of IC transcripts, resulting in the establishment and/or maintenance of imprinting in the *Snrpn* locus.

Acknowledgements

T.K. was supported in part by a Grant-in-Aid for Scientific Research (C) and that on Priority Areas from the Ministry of Education, Culture, Sports, Science and Technology of Japan. T.K. and M.K were supported in part by a Grant-in-Aid for Scientific Research from Nagasaki University, Japan.

References

Bourc'his, D., Xu, G.L., Lin, C.S., Bollman, B., Bestor, T.H., 2001. Dnmt3L and the establishment of maternal genomic imprints. Science 294, 2536–2539.
Constancia, M., Pickard, B., Kelsey, G., Reik, W., 1998. Imprinting mechanisms. Genome Res. 8, 881–900.
Dittrich, B., et al., 1996. Imprint switching on human chromosome 15 may involve alternative transcripts of the *SNRPN* gene. Nat. Genet. 14, 163–170.
El-Maarri, O., et al., 2001. Maternal methylation imprints on human chromosome 15 are established during or after fertilization. Nat. Genet. 27, 341–344.
Gabriel, J.M., Gray, T.A., Stubbs, L., Saitoh, S., Ohta, T., Nicholls, R.D., 1998. Structure and function correlations at the imprinted mouse Snrpn locus. Mamm. Genome. 9, 788–793.
Geuns, E., De Rycke, M., Van Steirteghem, A., Liebaers, I., 2003. Methylation imprints of the imprint control region of the SNRPN-gene in human gametes and preimplantation embryos. Hum. Mol. Genet. 12, 2873–2879.
Glenn, C.C., et al., 1996. Gene structure, DNA methylation, and imprinted expression of the human SNRPN gene. Am. J. Hum. Genet. 58, 335–346.
Hata, K., Okano, M., Lei, H., Li, E., 2002. Dnmt3L cooperates with the Dnmt3 family of de novo DNA methyltransferases to establish maternal imprints in mice. Development, 129, 1983–1993.
Hershko, A., Razin, A., Shemer, R., 1999. Imprinted methylation and its effect on expression of the mouse Zfp127 gene. Gene, 234, 323–327.
Johnstone, A., DuBose, A.J., Futtner, C.R., Elmore, M.D., Brannan, C.I., Resnick, J.L., 2006. A human imprinting centre demonstrates conserved acquisition but diverged maintenance of imprinting in a mouse model for Angelman syndrome imprinting defects. Hum. Mol. Genet. 15, 393–404.
Lucifero, D., Mertineit, C., Clarke, H.J., Bestor, T.H., Trasler, J.M., 2002. Methylation dynamics of imprinted genes in mouse germ cells. Genomics 79, 530–538.
Mapendano, C.K., et al., 2006. Expression of the Snurf-Snrpn IC transcript in the oocyte and its putative role in the imprinting establishment of the mouse 7C imprinting domain. J. Hum. Genet. 51, 236–243.
Nicholls, R.D., Knepper, J.L., 2001. Genome organization, function, and imprinting in Prader-Willi and Angelman syndromes. Annu. Rev. Genomics Hum. Genet. 2, 153–175.
Rodriguez-Jato, S., Nicholls, R.D., Driscoll, D.J., Yang, T.P., 2005. Characterization of cis- and trans-acting elements in the imprinted human SNURF-SNRPN locus. Nucleic Acids Res. 33, 4740–4753.
Schweizer, J., Zynger, D., Francke, U., 1999. In vivo nuclease hypersensitivity studies reveal multiple sites of parental origin-dependent differential chromatin conformation in the 150 kb SNRPN transcription unit. Hum. Mol. Genet. 8, 555–566.
Shemer, R., Birger, Y., Riggs, A.D., Razin, A., 1997. Structure of the imprinted mouse Snrpn gene and establishment of its parental-specific methylation pattern. Proc. Natl Acad. Sci. USA 94, 10267–10272.
Smith, K.T., Coffee, B., Reines, D., 2004. Occupancy and synergistic activation of the FMR1 promoter by Nrf-1 and Sp1 in vivo. Hum. Mol. Genet. 13, 1611–1621.
Surani, M.A., 1998. Imprinting and the initiation of gene silencing in the germ line. Cell 93, 309–312.
Tilghman, S.M., 1999. The sins of the fathers and mothers: genomic imprinting in mammalian development. Cell 96, 185–193.
Yamasaki, Y., et al., 2005. Neuron-specific relaxation of Igf2r imprinting is associated with neuron-specific histone modifications and lack of its antisense transcript Air. Hum. Mol. Genet. 14, 2511–2520.
Yoshida, K., et al., 1995. The modified method of two-step differential extraction of sperm and vaginal epithelial cell DNA from vaginal fluid mixed with semen. Forensic Sci. Int. 72, 25–33.

RESEARCH ARTICLE

AMERICAN JOURNAL OF
medical genetics

A Locus for Ophthalmo-Acromelic Syndrome Mapped to 10p11.23

Haruka Hamanoue,[1,2] Andre Megarbane,[3] Takaya Tohma,[4] Akira Nishimura,[1] Takeshi Mizuguchi,[1] Hirotomo Saitsu,[1] Haruya Sakai,[1] Shoko Miura,[5] Tatsushi Toda,[6] Noriko Miyake,[1] Norio Niikawa,[5] Koichiro Yoshiura,[5] Fumiki Hirahara,[2] and Naomichi Matsumoto[1]*

[1]Department of Human Genetics, Yokohama City University Graduate School of Medicine, Yokohama, Japan

[2]Department of Obstetrics and Gynecology, Yokohama City University Graduate School of Medicine, Yokohama, Japan

[3]Medical Genetics Unit, St. Joseph University, Beirut, Lebanon

[4]Division of Pediatrics, Okinawa Prefectural Nanbu Medical Center & Children's Medical Center, Haebaru, Japan

[5]Department of Human Genetics, Nagasaki University Graduate School of Biomedical Sciences, Nagasaki, Japan

[6]Division of Clinical Genetics, Department of Medical Genetics, Osaka University Graduate School of Medicine, Suita, Japan

Received 29 July 2008; Accepted 10 October 2008

Ophthalmo-acromelic syndrome (OAS, OMIM %206920) is a rare autosomal recessive disease, presenting with clinical anophthalmia and limb anomalies. We recruited three OAS families including a Japanese family with two affected patients and two consanguineous Lebanese families each having an affected. Homozygosity mapping was performed using the 50K SNP chip and additional informative markers. A locus for OAS was mapped to the 422-kb region at 10q11.23, based on the results from the two consanguineous families as well as the consistent data from the Japanese non-consanguineous family. The 422-kb region only contained one gene, *MPP7*. Although we could not detect any pathological mutations in OAS families analyzed, *MPP7* could remain a candidate as aberrant changes might exist beyond our mutation detection methods. Further families are needed to confirm this candidate locus. © 2009 Wiley-Liss, Inc.

Key words: ophthalmo-acromelic syndrome; linkage study; genetic locus; 10p11.23

How to Cite this Article:
Hamanoue H, Megarbane A, Tohma T, Nishimura A, Mizuguchi T, Saitsu H, Sakai H, Miura S, Toda T, Miyake N, Niikawa N, Yoshiura K, Hirahara F, Matsumoto N. 2009. A locus for ophthalmo-acromelic syndrome mapped to 10p11.23.
Am J Med Genet Part A 149A:336–342.

INTRODUCTION

Ophthalmo-acromelic syndrome (OAS, OMIM %206920), also known as Waardenburg's recessive anophthalmia syndrome, is a rare autosomal recessive disorder, presenting with anophthalmia or microphthalmia and limb anomalies. Since the first report by Waardenburg [1961], at least 35 cases from 21 families have been reported [Richieri-Costa et al., 1983; Pallotta and Dallapiccola, 1984; Traboulsi et al., 1984; Le Merrer et al., 1988; al Gazali et al., 1994; Quarrell, 1995; Sayli et al., 1995; Suyugul et al., 1996; Megarbane et al., 1998; Cogulu et al., 2000; Tekin et al., 2000; Caksen et al., 2002; Kara et al., 2002; Garavelli et al., 2006; Teiber et al., 2007]. Majority of OAS families are consanguineous (~90%) [Garavelli et al., 2006]. Ocular phenotypes in OAS widely range from mild microphthalmia to true anophthalmia [Kara et al., 2002]. Typical limb malformations include fused 4th and 5th metacarpals and short 5th finger in hands and olygodactyly in foot (four toes) [Teiber et al., 2007]. Most cases have bilateral anophthalmia/microphthalmia (88%), but unilateral abnormality is also noted. Other (visceral) malformations are rare, but venous or vertebral anomaly was recognized each in single cases [Tekin et al., 2000; Teiber et al., 2007].

The genetic cause for OAS remains undetermined. Genome-wide homozygosity mapping was undertaken and a locus for OAS was identified using three families including four affected individuals. A possible responsible gene will be discussed.

Grant sponsor: Ministry of Health, Labour and Welfare; Grant sponsor: SORST; Grant sponsor: Scientific Research from the Ministry of Education, Sports, Science and Technology, Japan.

*Correspondence to:
Naomichi Matsumoto, M.D., Ph.D, Department of Human Genetics, Yokohama City University Graduate School of Medicine, Fukuura 3-9, Kanazawa-ku, Yokohama 236-0004, Japan.
E-mail: naomat@yokohama-cu.ac.jp

Published online 10 February 2009 in Wiley InterScience (www.interscience.wiley.com)
DOI 10.1002/ajmg.a.32656

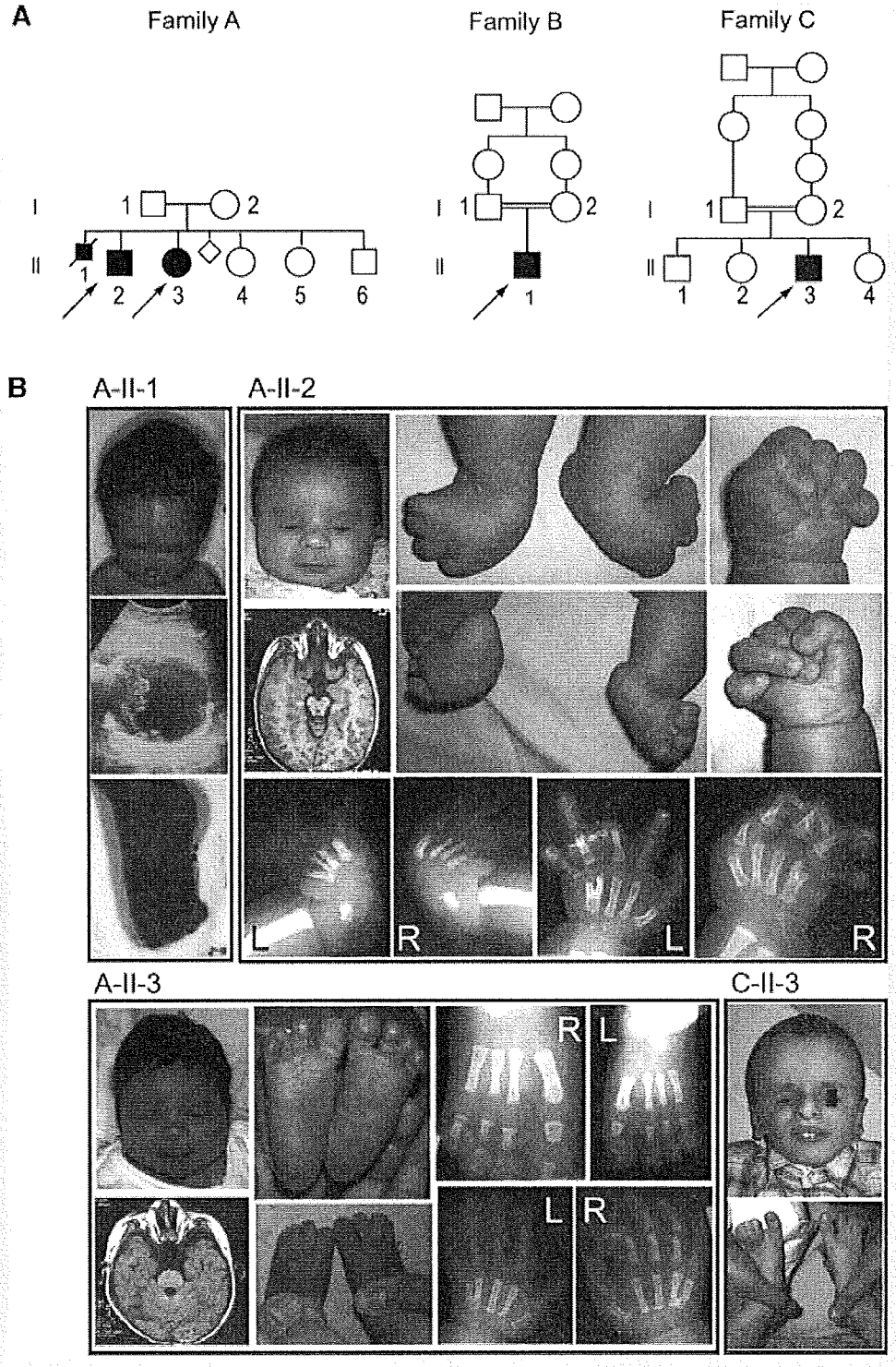

FIG. 1. Three OAS families used for this study and clinical manifestations of families A and C. A: Three OAS-family pedigrees are shown. Family A (Japanese) has two affected individuals and one affected abortus, family B (Lebanese) one affected born from the consanguineous parents, and family C (Lebanese) one affected also from the consanguineous parents. B: Clinical features of one affected abortus (A-II-1) and two affected individuals (A-II-2 and A-II-3) in family A and an affected individual (C-II-3) in family C. A-II-1 showed bilateral microphthalmia, adherent eyelids, bilateral oligodactyly (absence of 1st toes), cleft lip/palate and holoprosencephaly with hydrocephaly. A-II-2 at age of 6 years and A-II-3 at 5 years both presented with bilateral anophthalmia (confirmed by brain MRI), closed eyelids and limb anomalies with bilateral metacarpal synostosis between the 4th and 5th fingers and bilateral oligodactyly (absence of 1st toes). C-II-3 at age of 2 years showed bilateral anophthalmia and distal limb abnormalities including bilateral syndactyly of 2nd to 5th toes with symphysis.

MATERIALS AND METHODS

Patients and Their Families

Three families with one or two cases of OAS were analyzed in this study (Fig. 1 and Table I). In family A, two affected sibs (A-II-2 at 6 years and A-II-3 at 5 years) both presented with bilateral anophthalmia, closed eyelids and limb anomalies with bilateral metacarpal synostosis between the 4th and 5th fingers and bilateral oligodactyly (absence of 1st toes). In this family, their first child was a stillborn son (A-II-1), who had bilateral microphthalmia, adherent eyelids, bilateral oligodactyly (absence of 1st toes), cleft lip/palate and holoprosencephaly with hydrocephaly. Though no evidence of consanguinity was obtained, their eight grandparents were all originated from the Okinawa island in Japan. The other two families (B and C) were independent consanguineous Lebanese families, of which the family B was previously reported [Megarbane et al., 1998]. The proband B-II-1, a 10-year-old boy, was the first child of healthy parents, presenting with bilateral anophthalmia, adherent eyelids, deeply set orbits, anteverted nares, normally positioned ears, a normal philtrum, thin lips, micrognathia, very short neck, narrow chest, bilateral upper limb anomalies (split hands: four digits on the right hand and two digits on the left), and six short toes on the right foot (right postaxial polydactyly) [Megarbane et al., 1998]. These limb abnormalities are atypical for OAS. The patient, C-II-3, a 2-year-old boy, showed bilateral anophthalmia and distal limb abnormalities including bilateral syndactyly of 2nd to 5th toes. A total of 4 affected and 12 unaffected members from the three families were analyzed. Genomic DNA was obtained from peripheral blood leukocytes using QuickGene 610-L (FUJIFILM, Tokyo, Japan) after informed consent. Experimental protocols were approved by the Institutional Review Board at Yokohama City University School of Medicine.

SNP Genotyping

Whole SNP genotyping was undertaken using the GeneChip™ Human Mapping 50K Array *Xbal* (Affymetrix, Inc., Santa Clara, CA) containing 58,625 SNPs (single nucleotide polymorphism) according to the manufacture's protocols. In brief, 250 ng DNA was digested with *Xba*l. The adaptors were ligated to the digested DNA, and the ligation-mediated PCR with single-primer was performed. PCR products were purified by microcon YM-100 (Millipore, Inc., Billerica, MA). The product was fragmented, end-labeled, and hybridized to an array. SNP markers on the chip are almost equally distributed in the whole genome, with mean marker-distances of

TABLE I. Clinical Features of OAS Patients

	A-II-1	A-II-2	A-II-3	B-II-1	C-II-3
Origin	Okinawa, Japan	Okinawa, Japan	Okinawa, Japan	Lebanon	Lebanon
Consanguinity	−	−	−	+	+
Sex	Male	Male	Female	Male	Male
Eye abnormality	+	+	+	+	+
Anophthalmia	Bilateral	Bilateral	Bilateral	Bilateral	Bilateral
Loss of optic nerve (CT)	n.c.	Bilateral	Bilateral	Bilateral	Bilateral
Loss of optic tract (CT)	n.c.	+	+	−	−
Upper limb abnormality	+	+	+	+	+
Oligodactyly	n.c.	−	−	Right oligodactyly/ left lobster-claw	−
Metacarpal synostosis	n.c.	4th and 5th fingers	4th and 5th fingers	2nd and 3rd fingers	−
Clinodactyly	+	+	−	+	+
Camptodactyly	n.c.	+	−	+	+
Single transverse palmar crease	n.c.	+	+	n.c.	−
Lower limb abnormality	+	+	+	+	+
Oligodactyly/polydactyly/syndactyly	Bilateral oligodactyly	Bilateral oligodactyly	Bilateral oligodactyly	Right polydactyly	Bilateral syndactyly
Metatarsal synostosis	n.c.	+	+	+	−
Tibia valga	n.c.	+	+ (mild)	n.c.	−
Hypoplastic fibula	n.c.	+	+ (mild)	n.c.	−
Abnormal cleavage between toes	n.c.	1st and 2nd toes	1st and 2nd toes	−	1st and 2nd toes
Dermal syndactyly	n.c.	2nd and 3rd toes	2nd and 3rd toes	−	2nd to 5th toes
Talipes valgus	−	+	−	+	−
Other					
Holoprosencephaly	+	−	−	−	−
Cleft palate	+	−	−	−	−
Failure to thrive	n.c.	+	+	+	+
Developmental retardation	n.c.	DQ = 10	DQ = 15	+	+
Cryptorchidism	n.c.	Right		−	n.c.

n.c., not confirmed.

23.6 kb and an average heterozygosity of 0.30 among African American, European, and Asian. SNP calling, signal intensity data, and Mendelian error in each pedigrees to exclude conflicted SNPs were checked using GCOS 1.2 (the GeneChip Operating Software) platform (Affymetrix) and the Batch analysis in GTYPE 4.0 (GeneChip Genotyping Analysis Software) (Affymetrix), with the default setting for mapping algorithm. CNAG (Copy Number Analyser for GeneChip) Ver. 2.0 was also used to validate copy number alterations as well as loss of heterozygosity (LOH).

Linkage Analysis

Multipoint linkage analysis using aligned SNPs was performed using ALLEGRO software [Gudbjartsson et al., 2000, 2005]. Two-point linkage analysis of candidate regions was also performed using the LINKAGE package, MLINK (FASTLINK software, ver. 5.1). In each program, autosomal recessive model of inheritance with complete penetrance and a disease allele frequency of 0.001 were applied.

Fine Mapping With Short Tandem Repeat Markers

Fine mapping of possible candidate regions using additional microsatellite markers was done as previously described [Kondo et al., 2004]. Most markers were designed according to the Marshfield genetic map (http://research.marshfieldclinic.org/genetics). If appropriate markers were not found, candidate di-, tri-, and tetranucleotide repeat markers were originally selected from regions of interest using the UCSC genome browser (March 2006 assembly), and PCR primers were designed with the Primer3 program.

TABLE II. Primer Information of Markers

Marker	Forward (5′ > 3′)	Reverse (5′ > 3′)	Fluorescence	Product size (bp)	Annealing temperature (°C)
D10S1653[a]	CCTTTGGATAAAGCCTCCT	TATCATTGTCTCATCCGGG	VIC	201–213	55
D10S1661[a]	ACGCTACTTGCCAGGTC	ATTGCTTCCCTGAGAGTGT	VIC	250–272	58
D10S1476[a]	TGACTAAACAGACCCAGACTTG	GAACGCATGTCCACCCTA	NED	250–266	62
D10S504[a]	TCAGGTATTTCTTCATAGCAG	TTCCCTTGCTCTGCAGCTT	NED	366–370	62
D10S1125[a]	TGGTGGCCTCTTACCTAG	CCATTTGTATGTGTTCTCTTGAG	NED	225–249	64
D10S466[a]	CTGGGCCACAGTGAGACT	TAGGTCATCTGGTCTTCCATAC	NED	120–140	60
D10S1734[a]	GCCTGGGTGACAGAGTGAGATTCTA	ACACACGTACACATGGGGTGGT	NED	163–189	64
D10S1789[a]	TTTCCCACTCCAGTGC	TCATAGATAGAGACCATTAGTTTCA	VIC	134–150	60
D10S1673[a]	CCAACCTGGATGACAGAGC	CTTACCCCCAACCAAAGGAC	VIC	198–216	64
D10S1747[a]	TGTAGACCAGTAGACCATGACAAAT	CCACAGTCAGATATAGTGTGCAA	FAM	117–123	64
STS1[c]	TGTCCATCTCTTCAAACACTGG	TCCTGGGAATAGCGTTCACT	NED	243	60
AFM290XE1[a]	ATTTTTGACATTGTCCCA	CTAAGCCCTAGCACCTTT	FAM	247	57
AFM295TH1[a]	TATTATACTCCAGCCGGGG	GGAGACTATTTACTTTGTGTCCTTG	FAM	130	63
STS2[c]	TGGATATGAAAAGGGGTGATAA	GGTCCAGATGGTACTCACACG	FAM	246	60
STS3[c]	TGGGCTGCACATTTATACCA	TGTGACCTGCTCCTCACAAG	FAM	169	60
STS4[c]	TGATGTGTGTGTATTTTGTGTGTG	ACTCTTTGCAGCATCCCAGT	FAM	226	60
STS5[c]	TCTGTGTGCAGCTCCTCAGT	ACCTGGACAGGATCATCTGG	NED	224	60
D10S572[a]	CAGTGATTTTAGACAGGGATTTTA	AATTATGATACTTATTGATGGGGA	NED	275–283	63
D10S2481[b]	TGGAAGTTATGGACCAGGAA	CCAATGTCCAGCTAAGTGAGG	VIC	312	60
D10S197[a]	ACCACTGCACTTCAGGTGAC	GTGATACTGTCCTCAGGTCTCC	FAM	161–173	55
STS6[c]	TGCATTTAAGGAGAATCAGTTG	GCAGTGACTGTTCAAGATTTTTGT	FAM	194	60
STS7[c]	TGAACTACTGCTCTCAAATCTGTGT	GGGACACAATGGCTTTGAAC	VIC	157	60
STS8[c]	TTGGATTTTATTTGAAAATTAGGG	TTGGTTGGCTGAATAACTTCC	FAM	213	60
STS9[c]	GCTAATCCAGAGATACCACCAGA	CCTAGTTTGCTGAGACTGTTGTG	NED	371	60
STS10[c]	CCCTAGAAGTATTTGAAGAAGTAGCA	TGTGGTGCTCTTTCCTGTGA	NED	108	60
STS11[c]	GCTCAGTGGGACAATTCATGT	GAATAATGCCCCCGAAAGAT	VIC	399	60
STS12[c]	GCTGTTGGCTGTGAGTTCAA	CCCTTGGGCTTGGACTAGAA	FAM	388	60
UT541[a]	ATGGGGGTAGAGGGTCTGG	CAGCCTGGGTGACAAAGTCT	NED	143–340	60
AFMB345YA9[a]	GGAACCTAAGGCATGTTGAT	CCAAGACCCTGTCTGAAAAA	FAM	151–171	60
GATA29G05[a]	TGCTTATATCCAGCTAATATAAATG	CCATGAGGTTTATTTTCCCC	FAM	108–172	60
AFM095ZH7[a]	TATATGCAGTTTGGGATGGG	ATTGGGCTGTGCCTACACTT	VIC	213–231	60
D10S208[a]	AGGTGACTGTTTTGGGGGAG	GAGTGTGGGGATGTTTTCAA	NED	170–186	55
AFM137XH4[a]	AACATCCATTTGGAGAATTAAAAT	TACAGTGTGATTGCACGACT	NED	171–183	60
AFM353TB5[a]	TCAGTGGGAACGTAAATCAG	AGCTGAATATTATTCCATTGTGAGT	NED	175	58
D10S196[a]	TTCAAAGGTGGAGACCCTTC	TTTTGGTCAGAATGGAGTGG	VIC	99–109	55

[a]Primers for known microsatellite marker.
[b]Primers for known microsatellite marker with our modification.
[c]Newly designed primers.

Fluorescent-labeled (either FAM, VIC, or NED) forward primers and tailed reverse primers were purchased from Applied Biosystems (Tokyo, Japan). PCR products for each marker were electrophoresed on ABI Prism Genetic Analyzer 3100 (Applied Biosystems), and analyzed using GeneMapper Software ver. 3.5 (Applied Biosystems). PCR was cycled 40 times at 94°C for 30 sec, at 55–64°C for 30 sec and at 72°C for 30 sec in a total volume of 10 μl, containing 30 ng of genomic DNA as a template, 0.5 μM of each primer, 200 μM of each dNTP, 1× ExTaq buffer and 0.25 U ExTaq (Takara Bio, Inc., Ohtsu, Japan). Haplotype blocks were constructed manually. The list of primers is presented in Table II.

Mutation Analysis of a Candidate Gene

All coding exons and exon-intron boundaries together with 5′- and 3′-untranslated regions of *MPP7* (Membrane protein, palmitoylated 7) were analyzed. PCR was cycled 35 times at 94°C for 30 sec, at 60°C for 30 sec and at 72°C for 30–90 sec in a total volume of 20 μl containing 30 ng of genomic DNA as a template, 0.5 μM of forward and reverse primers, 200 μM of each dNTP, 1× ExTaq buffer, and 0.25 U of ExTaq (Takara Bio, Inc.). All primers were designed using the Primer3 software. Detailed information of *MPP7* primers is available on request. PCR products were purified with ExoSAP™ (USB Co., Cleveland, OH) and sequenced using BigDye Terminator 3.1 (Applied Biosystems) on the 3100 Genetic Analyzer. Sequences of patients were compared to the reference genome sequences in the UCSC Genome Browser (Mar 2006 assembly) using the Seqscape software ver. 2.1 (Applied Biosystems).

Expression Study of Mpp7 in Mouse Tissues

Whole head tissues from mice embryos at E10.5, eyeball, forelimb and hindlimb tissues from embryos each at E12.5, 13.5, and 16.5 were collected. Total RNA was extracted from collected tissues using Trizol reagent (Invitrogen, Carlsbad, CA). Two micrograms of RNA was reverse-transcribed in a volume of 20 μl using PrimeScript 1st strand cDNA Synthesis kit (Takara Bio, Inc). RT-PCR analysis was started at 94°C for 5 min as a first denaturing step, then cycled 25, 30, or 35 times at 94°C for 30 sec, at 56°C for 30 sec and at 72°C for 30 sec in a volume of 25 μl, containing 2 μl of reverse transcription reaction as a template, 0.2 μM of each primer, 400 μM of each dNTP, 1× ExTaq buffer and 0.125 U ExTaqHS (Takara Bio, Inc). Primers for RT-PCR were as follows: *Mpp7*-1-F, 5′-TGTATGAGCTGTTGGCTGCT-3′, and *Mpp7*-1-R, 5′-AGCCTT-

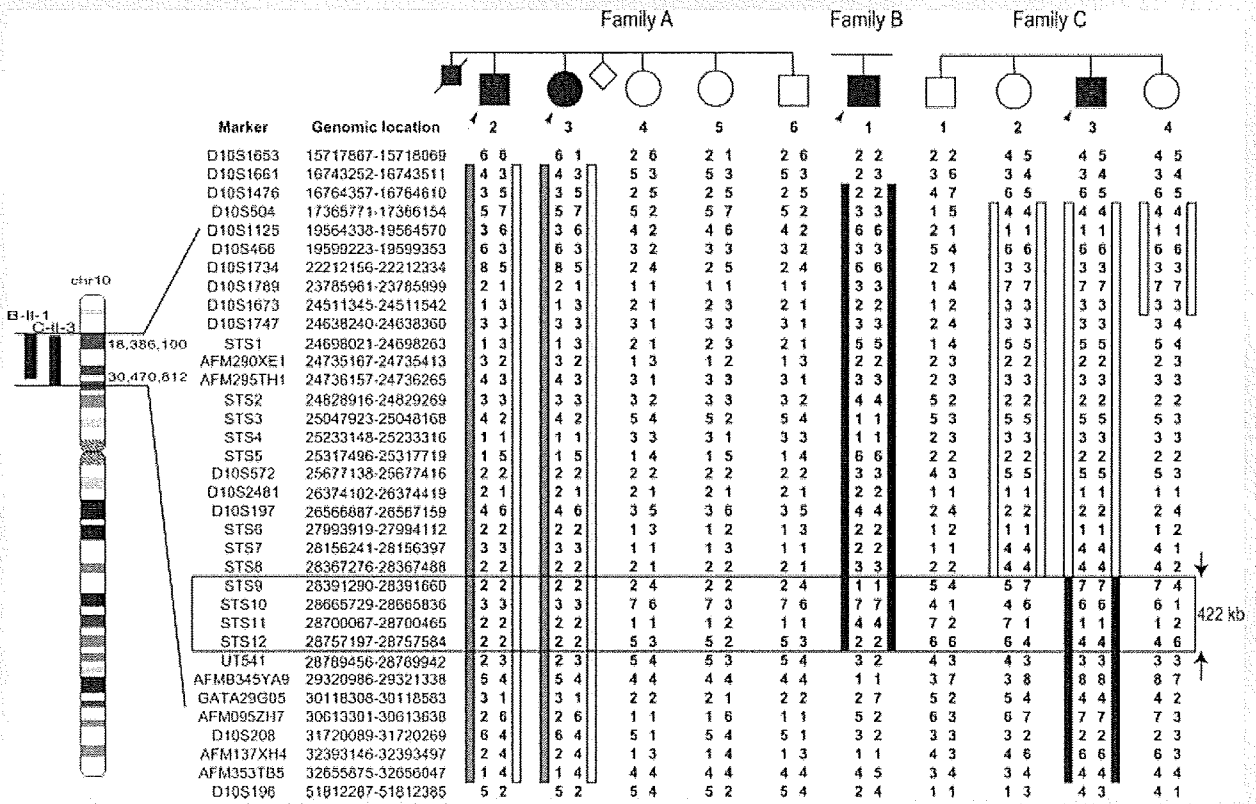

FIG. 2. Homozygosity mapping and haplotypes of three OAS families. Pedigrees of the three OAS families (Top). Chromosome 10 ideogram and IBD regions of B-II-1 and C-II-3 revealed by Affymetrix GeneChip 50K array are indicated with black bars. Polymorphic markers around IBD regions and haplotypes are indicated in all families. In families B and C, the common IBD region was mapped to a 422-Kb region, flanked by marker *STS8* and *UT541*. Affected sibs in Family A (II-2 and II-3) possess heterozygous haplotype blocks (shown as gray bars), probably implying compound heterozygous mutations.

GACATTGGGTTTTG-3′; *Mpp7*-2-F, 5′-AGCCTTGACATTGGG-TTTTG-3′, and *Mpp7*-2-R, 5′-TTATGAATGTAACCAACTCAC-TGG-3′. To ensure equal loading of cDNA into RT-PCR reactions, *B2m* cDNA was amplified as an internal control using the following primers: *B2m*-F, 5′-TGGTGCTTGTCTCACTGACC-3′, and *B2m*-R, 5′-TGCTTAACTCTGCAGGCGTAT-3′.

RESULTS AND DISCUSSION

Linkage analysis using ALLEGRO program revealed 16 candidate loci showing the LOD score ($\theta = 0.000$) higher than 3.0 (data not shown). All candidate regions except for a region of chromosome 10 (SNP blocks from rs7920803 to rs7094225 with the maximum LOD score, 3.9880) were ruled out by additional microsatellite markers as they did not show a pattern of identical by descent (IBD). LOH analysis using the CNAG program confirmed that B-II-1 and C-II-3 shared only one consistent region at chromosome 10. The region was comprised of 303 consecutive SNPs from rs1986480 to rs10508745, spanning approximately an 11-Mb segment at 10p12.33–p11.23 (Fig. 2). In contrast, A-II-2 and A-II-3 did not show any blocks of IBD, suggesting that it is unlikely that that their parents had a common ancestor. Further fine mapping using more markers confirmed that an affected individual (C-II-3) and an unaffected individual (C-II-2) shared the same homozygous genotype's region from *D10S504* to *STS8*. Thus the candidate region was narrowed down to a 422-kb segment from *STS9* and *STS12* at 10p11.23 through the analysis of families B and C. ALLEGRO program using all families indicated the maximum multi-point LOD score was 3.9863 near *STS9*. MLINK showed a maximum two-point LOD score was 2.9444 ($\theta = 0.000$) at *STS10*. Within the 422-kb region, only one established gene, *MPP7* (palmitoylated membrane protein 7) was located. Mutation screening of *MPP7* could not detect any abnormalities. All the haplotypes of the 422-kb segment in the three families are different.

Homozygosity mapping of two consanguineous Lebanese families each having an affected child revealed a candidate locus from *STS9* to *STS12*, a 422-kb region under the hypothesis that OAS is an autosomal recessive disorder. Though we initially expected that broad and many chromosomal regions might be highlighted as IBD, only a narrow 10p11.23 segment turned out to be a region of interest. Two affected sibs (A-II-1 and A-II-2) were likely to have less and smaller IBD regions as the family was not consanguineous. Indeed, we could not confirm any IBD regions on the Affymetrix 50K SNPs, suggesting that the two patients in the family A have compound heterozygous mutations.

Although *MPP7* is the only gene mapped to the 440-kb region and *Mpp7* is expressed in head tissues at E10.5, and in eyeballs and limbs at E12.5–E16.5 (Fig. 3), no causative mutations were found in our patients. This could be due to the limit of analytical methods. For example, mutations of promoter regions or small intragenic deletions/duplications might not be detected, though the Affymetrix GeneChip 50K could not detect any copy number changes of the region. Further investigation is absolutely necessary.

OAS is a very rare syndrome, usually the eye sign is consistent but the limb abnormalities are variable, so it is possible that OAS may have locus heterogeneity with different subtypes. As families B and

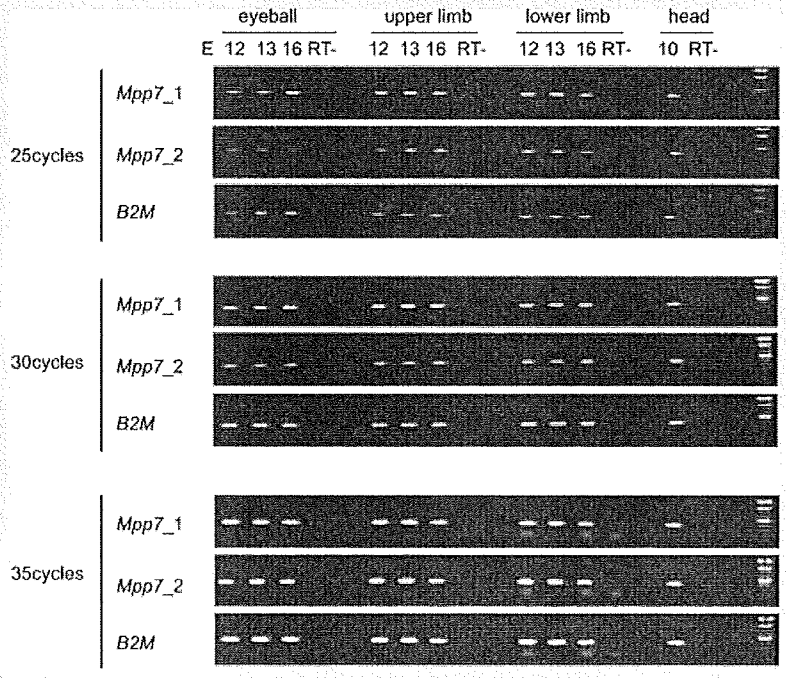

FIG. 3. Mpp7 expression analysis in mice embryonic tissues. *Mpp7* expression is confirmed using two different primer sets in all tissues examined by 25-, 30-, 35-cycled RT-PCR. Eyeball, upper and lower limb tissues at E12.5, E13.5, and E16.5, and whole head tissues at E10.5 were examined. *B2M* is an internal control gene.

C are of the same ethnic origin and were clinically examined by one of coauthors (M.A), we expected the similar haplotype for the two families. However, haplotypes of the 422-kb homozygous region are different between the two families. Thus the two families may not be caused by the same ancestral mutation. More families, if available, should be investigated.

In conclusion, a locus for OAS is validated by SNP homozygosity mapping. It is a 422-kb segment at 10p11.23 corresponding to *MPP7*, but no mutation was found. The SNP homozygosity mapping is very useful for autosomal recessive traits even if only a few families are available for study, but of course, more patients and families are definitely useful for this type of analysis.

ACKNOWLEDGMENTS

Patients and their families, all the collaborating doctors are highly appreciated. Research Grants from the Ministry of Health, Labour and Welfare (N.M.); SORST from JST (N.M. and N.N.); and Grant-in-Aid for Scientific Research from the Ministry of Education, Sports, Science and Technology, Japan (N.M.)

REFERENCES

al Gazali LI, Sabarinathan DK, Khidir A. 1994. Microphthalmia and distal limb abnormalities in a child of consanguineous parents. Clin Dysmorphol 3:258–262.

Caksen H, Odabas D, Oner AF, Abuhandan M, Calebi V. 2002. Ophthalmo-acromelic syndrome in a Turkish infant: Case report. East Afr Med J 79:339–340.

Cogulu O, Ozkinay F, Gunduz C, Sapmaz G, Ozkinay C. 2000. Waardenburg anophthalmia syndrome: Report and review. Am J Med Genet 90:173–174.

Garavelli L, Pedori S, Dal Zotto R, Franchi F, Marinelli M, Croci GF, Bellato S, Ammenti A, Virdis R, Banchini G, Superti-Furga A. 2006. Anophthalmos with limb anomalies (Waardenburg opththalmo-acromelic syndrome): Report of a new Italian case with renal anomaly and review. Genet Couns 17:449–455.

Gudbjartsson DF, Jonasson K, Frigge ML, Kong A. 2000. Allegro, a new computer program for multipoint linkage analysis. Nat Genet 25:12–13.

Gudbjartsson DF, Thorvaldsson T, Kong A, Gunnarsson G, Ingolfsdottir A. 2005. Allegro version 2. Nat Genet 37:1015–1016.

Kara F, Yesildaglar N, Tuncer RA, Semerci N, Onat N, Yilmazer YC, Sipahi T, Erkaya S. 2002. A case report of prenatally diagnosed ophthalmo-acromelic syndrome type Waardenburg. Prenat Diagn 22:395–397.

Kondo H, Qin M, Mizota A, Kondo M, Hayashi H, Hayashi K, Oshima K, Tahira T, Hayashi K. 2004. A homozygosity-based search for mutations in patients with autosomal recessive retinitis pigmentosa, using microsatellite markers. Invest Ophthalmol Vis Sci 45:4433–4439.

Le Merrer M, Nessmann C, Briard ML, Maroteaux P. 1988. Ophthalmo-acromelic syndrome. Ann Genet 31:226–229.

Megarbane A, Souraty N, Tamraz J. 1998. Ophthalmo-acromelic syndrome (Waardenburg) with split hand and polydactyly. Genet Couns 9:195–199.

Pallotta R, Dallapiccola B. 1984. A syndrome with true anophthalmia, hand-foot defects and mental retardation. Ophthalmic Paediatr Genet 4:19–23.

Quarrell OW. 1995. Ophthalmo acromelic syndrome. Clin Dysmorphol 4:272–273.

Richieri-Costa A, Gollop TR, Otto PG. 1983. Brief clinical report: Autosomal recessive anophthalmia with multiple congenital abnormalities–type Waardenburg. Am J Med Genet 14:607–615.

Sayli BS, Akarsu AN, Altan S. 1995. Anophthalmos-syndactyly (Waardenburg) syndrome without oligodactyly of toes. Am J Med Genet 58:18–20.

Suyugul Z, Seven M, Hacihanefioglu S, Kartal A, Suyugul N, Cenani A. 1996. Anophthalmia-Waardenburg syndrome: A report of three cases. Am J Med Genet 62:391–397.

Teiber ML, Garrido JA, Barreiro CZ. 2007. Ophthalmo-acromelic syndrome: Report of a case with vertebral anomalies. Am J Med Genet Part A 143A:2460–2462.

Tekin M, Tutar E, Arsan S, Atay G, Bodurtha J. 2000. Ophthalmo-acromelic syndrome: Report and review. Am J Med Genet 90:150–154.

Traboulsi EI, Nasr AM, Fahd SD, Jabbour NM, Der Kaloustian VM. 1984. Waardenburg's recessive anophthalmia syndrome. Ophthalmic Paediatr Genet 4:13–18.

Waardenburg PJ. 1961. Autosomally-recessive anophthalmia with malformations of the hand and feet. Genet Ophthalmol 772.

Journal of Human Genetics (2009), 1–6

www.nature.com/jhg

ORIGINAL ARTICLE

Molecular karyotyping in 17 patients and mutation screening in 41 patients with Kabuki syndrome

Hideo Kuniba[1,2,14], Koh-ichiro Yoshiura[1,14], Tatsuro Kondoh[2], Hirofumi Ohashi[3,14], Kenji Kurosawa[4], Hidefumi Tonoki[5], Toshiro Nagai[6,14], Nobuhiko Okamoto[7], Mitsuhiro Kato[8], Yoshimitsu Fukushima[9,14], Tadashi Kaname[10,14], Kenji Naritomi[10,14], Tadashi Matsumoto[2], Hiroyuki Moriuchi[2], Tatsuya Kishino[11,14], Akira Kinoshita[1,14], Noriko Miyake[12,14], Naomichi Matsumoto[12,14] and Norio Niikawa[1,13,14]

The Kabuki syndrome (KS, OMIM 147920), also known as the Niikawa–Kuroki syndrome, is a multiple congenital anomaly/mental retardation syndrome characterized by a distinct facial appearance. The cause of KS has been unidentified, even by whole-genome scan with array comparative genomic hybridization (CGH). In recent years, high-resolution oligonucleotide array technologies have enabled us to detect fine copy number alterations. In 17 patients with KS, molecular karyotyping was carried out with GeneChip 250K NspI array (Affymetrix) and Copy Number Analyser for GeneChip (CNAG). It showed seven copy number alterations, three deleted regions and four duplicated regions among the patients, with the exception of registered copy number variants (CNVs). Among the seven loci, only the region of 9q21.11-q21.12 (~1.27 Mb) involved coding genes, namely, transient receptor potential cation channel, subfamily M, member 3 (*TRPM3*), Kruppel-like factor 9 (*KLF9*), structural maintenance of chromosomes protein 5 (*SMC5*) and MAM domain containing 2 (*MAMDC2*). Mutation screening for the genes detected 10 base substitutions consisting of seven single-nucleotide polymorphisms (SNPs) and three silent mutations in 41 patients with KS. Our study could not show the causative genes for KS, but the locus of 9q21.11-q21.12, in association with a cleft palate, may contribute to the manifestation of KS in the patient. As various platforms on oligonucleotide arrays have been developed, higher resolution platforms will need to be applied to search tiny genomic rearrangements in patients with KS.
Journal of Human Genetics advance online publication, 3 April 2009; doi:10.1038/jhg.2009.30

Keywords: Kabuki syndrome; microdeletion; molecular karyotyping; mutation screening; Niikawa–Kuroki syndrome

INTRODUCTION

Kabuki syndrome (KS, OMIM 147920), also known as Niikawa–Kuroki syndrome, is a multiple congenital anomaly/mental retardation (MCA/MR) syndrome characterized by a distinct facial appearance, skeletal abnormalities, joint hypermobility, dermatoglyphic abnormalities, postnatal growth retardation, recurrent otitis media and occasional visceral anomalies.[1,2] The prevalence was estimated to be 1/32 000 in Japan[3] and 1/86 000 in Australia and New Zealand.[4] Although most cases were sporadic, at least 14 familial cases have been reported. It is assumed that KS is an autosomal dominant disorder, considering the equal male-to-female ratio of patients and parent–child transmission pattern in some familial cases.[5]

The cause of KS remains unknown, even though at least 400 patients have been diagnosed in a variety of ethnic groups since 1981.[3–7] Some works have ruled out several loci; for example, 1q32–q41, 8p22–p23.1 and 22q11, as candidates for KS.[8–13] A study of array-based comparative genomic hybridization (CGH) showed a disruption of the *C20orf133(MACROD2)* gene by ~250 kb deletion in a patient with KS,[14] but the following mutation screening for the gene failed to find a pathogenic base change within exons in 19 other patients with KS[14] and in 43 Japanese patients.[15] Another study of array CGH with 0.5–1.2 Mb resolution reported that 2q37 deletions were detected in two patients with Kabuki-like features, but their facial features were not typical for KS.[16] To date, no concordant specific lesion has been

[1]Department of Human Genetics, Nagasaki University Graduate School of Biomedical Sciences, Nagasaki, Japan; [2]Department of Pediatrics, Nagasaki University School of Medicine, Nagasaki, Japan; [3]Division of Medical Genetics, Saitama Children's Medical Center, Iwatsuki, Japan; [4]Division of Medical Genetics, Kanagawa Children's Medical Center, Yokohama, Japan; [5]Department of Pediatrics, Tenshi Hospital, Sapporo, Japan; [6]Department of Pediatrics, Dokkyo University School of Medicine Koshigaya Hospital, Koshigaya, Japan; [7]Department of Planning and Research, Osaka Medical Center and Research Institute for Maternal and Child health, Osaka, Japan; [8]Department of Pediatrics, Yamagata University School of Medicine, Yamagata, Japan; [9]Department of Medical Genetics, Shinshu University School of Medicine, Matsumoto, Japan; [10]Department of Medical Genetics, University of the Ryukyus, Nishihara, Japan; [11]Division of Functional Genomics, Center for Frontier Life Sciences, Nagasaki University, Nagasaki, Japan; [12]Department of Human Genetics, Yokohama City University Graduate School of Medicine, Yokohama, Japan; [13]Research Institute of Personalized Health Sciences, Health Sciences University of Hokkaido, Tobetsu, Japan and [14]Solution Oriented Research for Science and Technology (SORST), Japan Science and Technology Agency (JST), Tokyo, Japan
Correspondence: Dr K-i Yoshiura, Department of Human Genetics, Nagasaki University Graduate School of Biomedical Sciences, Sakamoto 1-12-4, Nagasaki 852-8523, Japan.
E-mail: kyoshi@nagasaki-u.ac.jp
Received 15 January 2009; revised 3 March 2009; accepted 11 March 2009

found by whole-genome scan with array CGH in a bacterial artificial chromosome (BAC) clone with 0.5–1.5 Mb resolution.[16–18]

Chromosomal aberration analysis by high-resolution oligonucleotide array technologies in recent years, called molecular karyotyping, enables us to detect submicroscopic pathogenic copy number alterations, which were undetectable even by BAC array CGH.[19,20] As not a few MCA/MR syndromes are because of chromosomal copy number aberration, we hypothesize that some sort of microdeletion/microduplication causes KS. Herein, we report the results of molecular karyotyping in 17 patients using GeneChip 250K array and those of mutation screening of candidate genes in 41 patients with KS in Japan.

MATERIALS AND METHODS

Subjects

The subjects for molecular karyotyping consisted of 18 patients (nine girls and nine boys) at entry. The subjects for mutation screening consisted of 41 patients (20 girls and 21 boys), including the aforementioned 18 patients. The diagnoses of KS were confirmed by experts of clinical genetics, although written permission for the use of facial photographs in publications was not obtained. These Japanese patients showed a normal karyotype at a 400-band level, and were earlier reported with no pathogenic genome copy number change by 1.5 Mb-resolution BAC array CGH.[18] Genomic DNA was isolated by the standard method from their peripheral blood leukocytes or in part from their lymphoblastoid cell lines. Experimental procedures were approved by the Committee for the Ethical Issues on Human Genome and Gene Analysis at Nagasaki University.

Molecular karyotyping

DNA oligomicroarray hybridization, using the GeneChip Human Mapping 250K Nsp Array (Affymetrix, Santa Clara, CA, USA), was carried out for 18 patients with KS, following the provided protocol (Affymetrix). Data were analyzed using GTYPE (GeneChip Genotyping Analysis Software) to detect copy number aberration and visualized using CNAG (Copy Number Analyser for GeneChip) version 3.[21] References for non-paired analysis of CNAG were chosen from eight unrelated individuals of HapMap samples from the Affymetrix website (http://www.affymetrix.com/support/). The resolution of this procedure was estimated as ~30–100 kb. CNAG version 3 was linked with the University of California Santa Cruz (UCSC) genome browser (http://genome.ucsc.edu/) assembly May 2004, and then its physical position was referred to the data assembly on March 2006 in the UCSC genome browser after adjustment.

Validation of deletion

Quantitative PCR (qPCR) analysis to validate deletions was run on a LightCycler 480 Real-Time PCR System (Roche Diagnostics, Mannheim, Germany) using an intercalating dye, SYTO9 (Molecular probes, OR, USA), which is an alternative to SYBR green I.[22] Absolute quantification was carried out using a second derivative max method. A standard curve of amplification efficiency for each set of primers was generated with a serial dilution of genomic DNA. A corrected gene dosage was given as the ratio of a target gene divided by an internal control gene. The copy number was obtained from a calibration under the assumption that the control genome was diploid.

Target genes of copy number aberration were as follows: *SUMF1* (for patient K9); *MAMDC2* (for patient K16); and *CETN1* (for patient K34). The primer sequences of these genes are available in the online supplementary file. Internal control diploid genes were *OAZ2* and *USP21*. Primer sets of the control genes for genomic DNA were selected from the Real Time PCR Primer Sets website (http://www.realtimeprimers.org/). The control genes were confirmed to have no copy number variants on the Database of Genomic Variants (DGV) updated on 26 June 2008 (http://projects.tcag.ca/variation/). BLAST searches confirmed all primer sequences specific for the gene.

Samples were analyzed in triplicate in a 384-well format in a 10 μl final volume containing about 2 ng genomic DNA, 0.5 μM forward primer, 0.5 μM reverse primer, 0.1 Units TaKaRa ExTaq HS version (TaKaRa, Kyoto, Japan), 1× PCR buffer, 200 μM dNTP and 0.5 μM SYTO9. The amplification conditions consisted of an initial denaturation at 95 °C for 5 min, followed by 45 cycles of

Table 1 Detected genomic copy number aberrations in 17 patients with Kabuki syndrome

Cytoband	*Patient(s) ID*	*CN State*	*Length*	*Physical position*		*Involving gene(s)*	*Concordant loss/gain on DGV*
				Start	*End*		
3p26.3	K7	1	460 kb	1435279	1895554	NR	Variation_8235
3p26.2	K9	1[a]	205 kb	4009368	4214847	*SUMF1*	Variation_8973, 8975, 30169
4q13.2	K23	1[a]	1.26 Mb	66329014	67591611	NR	NR
5q21.2-q21.3	K22	1	281 kb	104301325	104581898	NR	Variation_3568
9q21.11-q21.12	K16	1[a]	1.27 Mb	71760296	73031176	*TRPM3, KLF9, SMC5, MAMDC2*	NR
14q11.2	K5	1	166 kb	19336854	19502641	*OR4N2, OR4K2, OR4K5, OR4K1*	Variation_0376, 7028, 8094, 9234, 9235
15q11.2	K1, K23	1	972 kb	19356830	20329239	*OR4M2, OR4N4, LOC65D137*	Variation_0318, 3070, 8265, 9251, 9254, 9256
18p11.32	K34	1[a]	35 kb	545074	580003	*CETN1*	Variation_5044
20p12.1	K6	1[a]	152 kb	14993412	15145890	*C20orf133 (MACROD2)*[b]	NR
4q12	K5	3	104 kb	54251599	54355281	NR	NR
8q11.21	K7	3	171 kb	50641101	50812548	NR	Variation_2751, 3731, 8601, 37765
10p15.2-p15.1	K5	3	142 kb	3663600	3805292	NR	NR
13q31.1	K6	3	72 kb	82451568	82523728	NR	NR
15q11.2	K7, K9, K12	3	877 kb	19112164	19989036	*CXADRP2, POTEB*	Variation_3070, 3951, 8784, 30670, etc.
15q25.1	K9	3	165 kb	76992181	77156751	*CTSH, RASGRF1*	Variation_3970, 7073
16q21	K13	3	283 kb	58508008	58791285	NR	NR
17q12	K7	3	495 kb	31428390	31923810	*CCL3, CCL4, CCL3L1, CCL3L3, CCL4L1, CCL4L2, TBC1D3B, TBC1D3C, TBC1D3G*	Variation_3142, 4031, 8841, 30824, etc.
22q11.22	K5, K12	3	278 kb	20907806	21186081	*VPREB1, ZNF280B*	Variation_5356, 34540

Abbreviations: CN, copy number; DGV, Database of Genomic Variants; NR, no registration in UCSC genes or DGV.
[a]Validated by quantitative PCR.
[b]Deleted region was within intron 5 of the *C20orf133 (MACROD2)* and did not involve any coding exon.[15]

denaturation at 95 °C for 10 s, annealing at 55 °C for 10 s and extension at 72 °C for 15 s The data were analyzed using LightCycler 480 Basic Software (Roche Diagnostics) and the melting curve was checked to eliminate non-specific products from the reaction.

Mutation screening of candidate genes

Candidate genes, identified within a detected deletion, consisted of four genes: *TRPM3* (NM_001007471 and NM_206946), *KLF9* (NM_001206), *SMC5* (NM_015110) and *MAMDC2* (NM_153267) located at 9q21.12–q21. 11. The entire coding region and splice junctions of the genes were sequenced on an automated sequencer 3130xl (Applied Biosystems, Foster City, CA, USA) using BigDye version 3.1 (Applied Biosystems). Genomic sequences were retrieved from the UCSC genome browser (assembly: March 2006). PCR primers were designed with the assistance of Primer3 (http://frodo.wi.mit.edu/cgi-bin/primer3/primer3.cgi). The primer sequences are available in the online supplementary file. Resultant electropherograms were aligned using ATGC version 3.0 (Software Development, Tokyo, Japan) and inspected visually to find DNA alterations.

In silico analysis

Relations among deleted genes were assessed using online software, PANTHER (Protein Analysis Through Evolutionary Relationships, http://www.pantherdb.org), to determine whether the genes involve some developmental pathway or biological process.[23] The novel synonymous base substitutions found in the mutation screening were examined for their potential activation of the cryptic splice site by comparison between wild-type allele and mutated allele using the GeneSplicer program (http://www.cbcb.umd.edu/software/GeneSplicer/gene_spl.shtml).

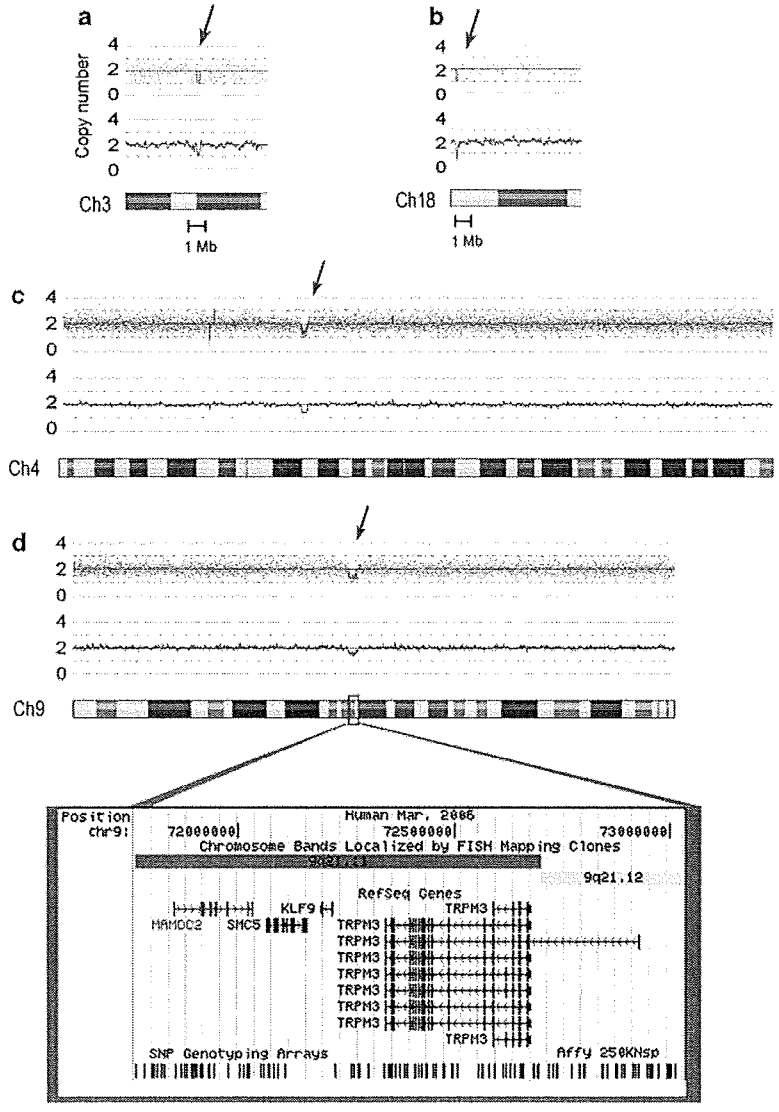

Figure 1 Chromosome view of Copy Number Analyser for GeneChip (CNAG) analysis. Each dots represent fluorescent intensity on each single-nucleotide polymorphisms (SNP) probe of GeneChip 250K NspI array (Affymetrix). Solid lines indicate copy number analyzed with CNAG. Arrows show detected deletions. (**a**) Chromosome (Ch) 3 of patient K9, ~205 kb deletion in 3p26.2 involving an exon of *SUMF1*gene. (**b**) Chromosome 18 of patient K34, ~35 kb deletion in 18p11.32, containing the *CETN1* gene. (**c**) Chromosome 4 of patient K23, ~1.26 Mb deletion in 4q13.2, not involving any known gene. (**d**) Chromosome 9 of patient K16, ~1.27 Mb deletion in 9q21.11–q21.12, harboring four genes: *TRPM3*, *KLF9*, *SMC5* and *MAMDC2*. The University of California Santa Cruz genome browser denotes the cytobands, genes and probe setting of Affymetrix 250K NspI array within the region. No copy number variation was registered here in the Database of Genomic Variants updated 26 June 2008. FISH, fluorescent *in situ* hybridization.